Gravure as an Industrially Viable Process for Printed Electronics

Vivek Subramanian
Donovan Sung

Electrical Engineering and Computer Sciences
University of California at Berkeley

Technical Report No. UCB/EECS-2008-70
http://www.eecs.berkeley.edu/Pubs/TechRpts/2008/EECS-2008-70.html

May 23, 2008

Gravure as an Industrially Viable Process for Printed Electronics

by Donovan Sung

Research Project

Submitted to the Department of Electrical Engineering and Computer Sciences, University of California at Berkeley, in partial satisfaction of the requirements for the degree of **Master of Science, Plan II**.

Approval for the Report and Comprehensive Examination:

Committee:

Professor Vivek Subramanian
Research Advisor

(Date)

* * * * * * *

Professor Nathan Cheung
Second Reader

(Date)

Gravure as an Industrially Viable Process

for Printed Electronics

By

Donovan Sung

Department of Electrical Engineering and Computer Sciences

University of California, Berkeley

Table of Contents

Abstract

In order for low-cost printed electronics to become ubiquitous, a suitable printing technique must be found. Gravure is a high-speed roll-to-roll printing technique which has many of the characteristics necessary for an industrially viable process for printed electronics. In gravure printing, an engraved cylinder is submerged in an ink fountain and then rolled over a flexible substrate such as plastic or paper. A tightly pressed blade, called the doctor blade, wipes off excess ink from the non-image areas of the cylinder surface before contact with the substrate. Gravure has the advantages of high throughput, long print runs, uniformity, and versatility.

We explore the construction of a gravure printing system, including the design of a laboratory size printer and cylinder making techniques. Industrial best practices are presented along with techniques discovered in the laboratory. We discuss the choice of cylinder material, as well as different metrics for determining acceptable cylinders. Next, we compare four methods of patterning cylinders and discuss challenges in scaling to an industrial printing system.

Next, we consider the theoretical considerations necessary to develop a printing process to deposit conductive lines less than 20 microns wide, suitable for bottom-gate thin film transistors (TFTs). We discuss the physical principles governing the gravure printing process, which can be separated into the two actions of cell emptying and drop spreading. We demonstrate gravure-printed nanoparticle lines and present techniques for optimizing the printed line quality by varying print parameters such as cell spacing and viscosity. Finally, we discuss possible routes to printed TFTs and future work.

Acknowledgements

I would like to thank my research advisor, Professor Vivek Subramanian, for his advice and support over the past two years. His expertise in various areas of engineering was very helpful in guiding the direction of this project, and I have learned to become a better scientist from my interactions with him. I would also like to thank Professor Nathan Cheung for giving me feedback and taking the time to read this report.

The members of the Organics Electronics Group supported me at various stages of this project, and without their help, this project would not have been possible. Our lab office was always a fun place to work, and I enjoyed the discussions we had about research, Starcraft, and other miscellaneous topics. In particular, I would like to thank Alejandro de la Fuente for teaching me from the very beginning and helping me every step of the way. He has not only been a great mentor, but also a valuable friend.

I would like to acknowledge the help of several industrial companies including WRE/Colortech, Rotadyne, GravurExchange, and Soligie. These companies provided much needed advice and expertise, and I had a rewarding experience working with them on this project.

Finally, I would like to thank my family and friends, especially Dianna, for their constant support and encouragement.

.

.

Chapter 1: Introduction

1.1 **Printed Electronics**

Low cost printed electronics promise to enable new applications such as RFID tags, displays and chemical sensors. Compared to traditional methods of manufacturing silicon integrated circuits, printing technology has several characteristics that may allow it to be both faster and cheaper. First, printing is a large area technique and allows for roll-to-roll processing on a variety of substrates, including paper and plastic. Second, printing is an all-additive process, so that no excess material is deposited and material and waste disposal costs can be reduced. Finally, printing does not require expensive equipment for vacuum processing, photolithography, and other expensive processes associated with traditional semiconductor manufacturing [Garnier].

To date, there have been no commercial all-printed electronic products. The biggest industrial successes have come from printing passive devices with only one layer of material. Both Avery Dennison and Omron have successfully utilized roll-to-roll printing of conductive silver flake ink for UHF-RFID antennas. At UHF, the requirements on antenna conductance and pattern fidelity are not very stringent [Harrop]. Additionally, researchers have printed spiral inductor coils and interdigital capacitors [Pudas].

There has been less success with printing active devices such as transistors, which require precise alignment of multiple layers. Each layer must be extremely smooth and uniform in height, so that it does not adversely affect the layer on top. Researchers have printed entire transistors using only mass-printing technologies such as gravure, flexography, and offset, but these transistors have large gate lengths of 100 microns and substantial overlap capacitance [Huebler, Zielke]. Additionally, only top-gate structures have been achieved because the printed gate lines are too rough to be used in bottom-gate structures. Top-gate structures tend to have worse mobilities than bottom-gate structures because the semiconducting layer is printed first and is subject to contamination from subsequent layers, which can degrade the transistor performance [Molesa]. Additionally, the semiconducting layer forms a better interface with the dielectric when the dielectric is printed first [Fritz].

Currently, inkjet printing is the most studied method of printing low-cost electronics. Inkjet has a number of advantages which make it a good research tool. Its main advantage is its real-time dynamic alignment, which is critical for printing transistors correctly. A process flow for formation of inkjet-printed thin film transistors (TFTs) is shown in Figure 1. This process flow is applicable to any bottom-gated TFT structure regardless of which printing technologies are used. First, a metallic gate layer is printed. This layer is typically composed of nanoparticles, which can be annealed to form a smooth, conductive gate. This is followed by a polymer dielectric, source/drain contacts, and a semiconducting layer for the channel [Subramanian]. If the source/drain contacts are not aligned with the gate during printing, then the transistor will exhibit undesirable behavior such as excessive series resistance.

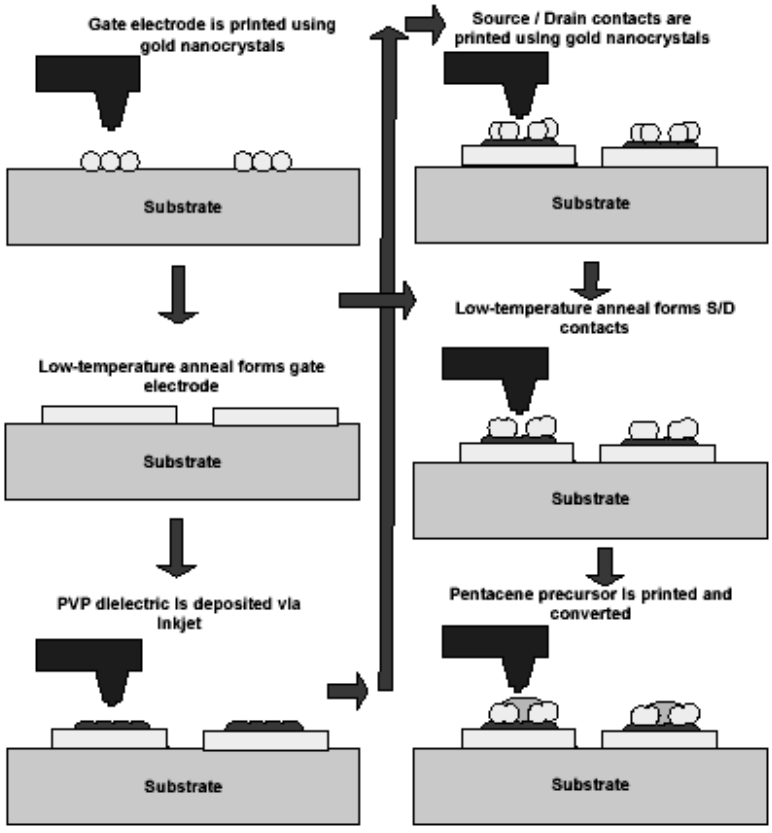

Figure 1. Process Flow for Formation of Inkjet Printed Transistors [Subramanian]

Despite the promising results, inkjet printing has a number of disadvantages which prevent it from becoming an industrial production technique for printed electronics. First, it has a low throughput because of its slow print speed. Each ink droplet must be individually deposited through a printing dispenser, as opposed to roll-to-roll printing techniques where multiple drops can be printed at the same time. Second, inkjet printing tends to have short run lengths because the print heads are subject to clogging. Third, it cannot easily print a wide range of ink viscosities, which is necessary to properly optimize printed lines. Finally, it has a certain level of process instability because of statistical variation of droplets.

1.2 Gravure Printing Technology

Gravure printing is a high-speed roll-to-roll printing technique which can overcome the disadvantages of inkjet and reproduce the process flow in Figure 1 with much higher throughput. Gravure is commonly used in the graphic arts industry for medium to long print runs where uniformity and versatility are required. Gravure printed products span a wide range, including bank notes, gift wrap, magazines, and postage stamps.

Gravure is an intaglio printing process, which means that the image carrier has the image etched below the surface of the non-image area. The gravure image carrier is an engraved cylinder patterned with individual wells that form a continuous image when printed. There are five main aspects of the gravure printing press: an engraved cylinder, doctor blade, ink fountain, impression roller, and drying press [GAA]. Figure 2 shows a schematic of a typical gravure printing process.

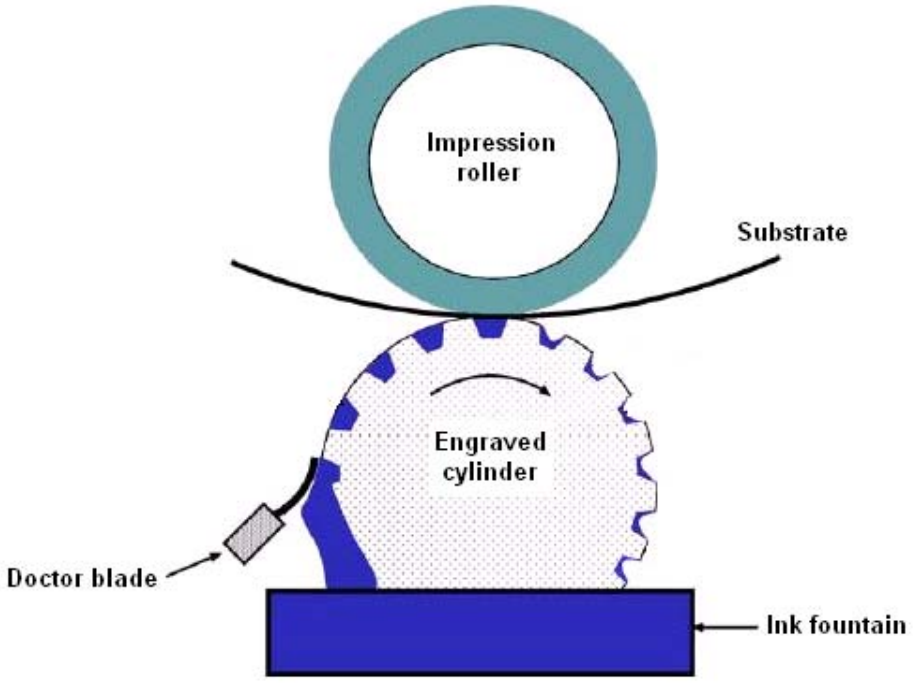

Figure 2. Schematic of Gravure Printing Process [Yin]

In gravure printing, the engraved cylinder is submerged in an ink fountain and then rolled over the substrate. A tightly pressed blade, called the doctor blade, wipes off excess ink from the non-image areas of the cylinder surface before contact with the substrate. The gravure cylinder most commonly consists of a steel core covered by a layer of copper, which is then patterned and covered with a thin layer of chrome to protect against wear from the doctor blade. The average lifetime for copper-chrome cylinders is between two to three million impressions, which is equivalent to a week of nonstop printing. Cylinders can be reused by stripping the chrome and copper layers. Modern engraving systems are capable of transferring digital images directly to the cylinder surface, which has helped to reduce the lead time for engravings to a few hours [GAA].

Gravure has a number of advantages over inkjet. First, gravure has a higher throughput because of its wider print area and its faster printing speed of up to 2000 ft/min. Gravure is also capable of simultaneously depositing multiple drops in a parallel fashion, as opposed to inkjet which must deposit drops one at a time in a serial fashion. Second, gravure can sustain long print runs because the cells are continuously refilled with ink as

the roll is rotated into the ink fountain, and the roll is not subject to clogging. Finally, gravure is a very versatile process capable of printing on a broad range of substrates with a wide range of ink viscosities. These advantages also help gravure compete against other high-speed printing processes such as flexography, letterpress, lithography, and screen printing. Gravure is a mechanically simple process with fewer controlling variables than other printing processes, which tends to give it a more consistent image quality.

1.3 Scope

The overall goal of this project is to develop a gravure printing system for manufacturing thin film transistors. In particular, this report will focus on two aspects of the printing process: a patterning process to render cells suitable for printed electronics, and a printing process to deposit conductive lines less than 20 microns wide, suitable for bottom gate structures. This report also provides insight into the science of the gravure printing process by examining the change in printed line quality as a function of cell and ink parameters. The independent variables are cell width, cell depth, cell spacing, and viscosity.

Chapter 2 explores the construction of a gravure printing system, including the design of a laboratory scale printer and cylinder making techniques. Four different patterning methods are discussed and compared. Chapter 3 describes theoretical considerations in the gravure printing process and establishes the experimental outline of this project. Techniques for optimizing printed gate lines are presented and possible routes to printed TFTs are discussed.

References

[Fritz] Fritz,S. E. “Structure and Transport in Organic Semiconductor Thin Films.” (PhD thesis, University of Minnesota, 2006)

[GAA] Gravure Education Foundation and Gravure Association of America. *Gravure: Process and Technology*. Versailles, KY. 2003.

[Garnier] Garnier, F. *et al.* 1994. “All-Polymer Field-Effect Transistor Realized by Printing Techniques.” *Science*, Vol 265. 1684-1686.

[Harrop] Harrop, P. “Flexo vs gravure: a battle to be repeated with printed electronics.” *IDTechEx.* April 6, 2006. http://www.idtechex.com/products/en/articles/00000465.asp

[Huebler] Huebler, A.C. *et al.* 2007. “Ring oscillator fabricated completely by means of mass-printing technologies.” *Organic Electronics,* 8, pp. 480-486.

[Molesa] Molesa, S. “Ultra-Low-Cost Printed Electronics.” (PhD thesis, University of California, Berkeley, 2006).

[Pudas] Pudas, M. *et al*. 2005. “Roller-type gravure offset printing of conductive inks for high-resolution printing on ceramic substrates.” *International Journal of Electronics,* Vol. 92, No. 5, 251-259.

[Subramanian] Subramanian, V*, et al.* 2005. “Progress Toward Development of All-Printed RFID Tags: Materials, Processes, and Devices.” *IEEE,* Vol. 93, No. 7, pp. 1330-1338.

[Yin] Yin, X. and S. Kumar. 2005. “Flow visualization of the liquid-emptying process in scaled-up gravure grooves and cells.” *Chemical Engineering Science,* 61:4:1146-1156.

[Zielke] Zielke, D. *et al*. 2005. “Polymer-based organic field-effect transistor using offset printed source/drain structures.” *Applied Physics Letters*, 87, 123508.

Chapter 2: Construction of Gravure Printing System

2.1 Design of Gravure Printer

This chapter will explore the construction of a laboratory gravure printing system. First, the laboratory printer will be described and compared to a typical industrial printer. Although the laboratory printer is relatively small, the basic principles of printing remain the same and the discovered trends should be transferable to larger printers as well. Next, techniques for cylinder making will be discussed. Topics include the choice of material, polishing, and patterning. Certain special considerations had to be taken into account because of the small size of the roll, and the techniques for scaling these to an industrial system will also be discussed.

The laboratory printer has several important design considerations. The printer is designed to be small enough in size to work as a laboratory scale printer, while still having the capability to reproduce the actual print conditions of an industrial printer. The printing process is designed to use only a small amount of ink per print, since much of the experimental work is conducted with silver nanoparticle inks which are more expensive than typical color inks. The printer is also designed with the ability to align successive prints within 2 microns, which is one to two orders of magnitude better than the industry standard of 50-100 microns.

The printer has an overall length of 1.5 meters and an overall height of 52 cm. It is mounted on an air sensitive table to protect against external vibrations. It has the ability to control print variables such as printing speed, blade angle, and blade pressure. The printing speed is controlled by a precision linear motor which has a maximum speed of 2.5 m/s. Commands are sent to the motor through a custom software interface. The doctor blade can be set at any angle between 0 to 90°. The blade pressure is controlled by a pneumatic switch and can be set from 0 to 160 pounds per square inch (psi). Three cameras are used as part of an alignment system, which will not be described in detail in this report. A model of the laboratory printer is shown in Figure 3.

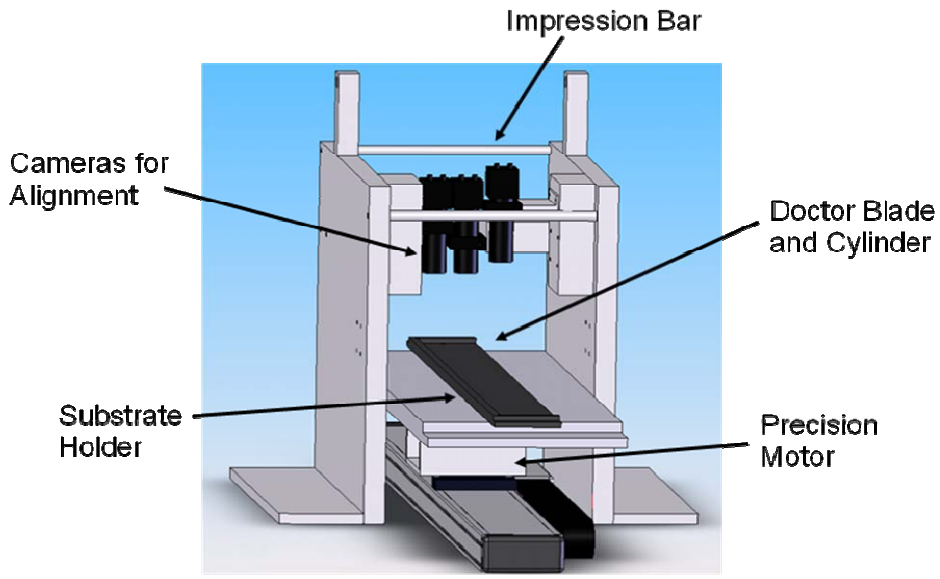

Figure 3. Model of Laboratory Gravure Printer [Source: Alejandro de la Fuente]

Figure 4 shows a schematic of the printing process for the laboratory gravure printer. The most striking difference between this process and a typical industrial process is the lack of an ink fountain and an impression roller. In order to minimize the ink used per print, the ink fountain was removed from the final design. During each print, ink is simply deposited at the nip, which is the intersection between the doctor blade and the cylinder. After each print, the cylinder and doctor blade are removed from the setup and cleaned. The impression roller has been replaced a flat substrate carrier covered by a hard rubber blanket, as is commonly done with most tabletop printers and pad printers. This printing process is similar to those used in industrial proofing presses.

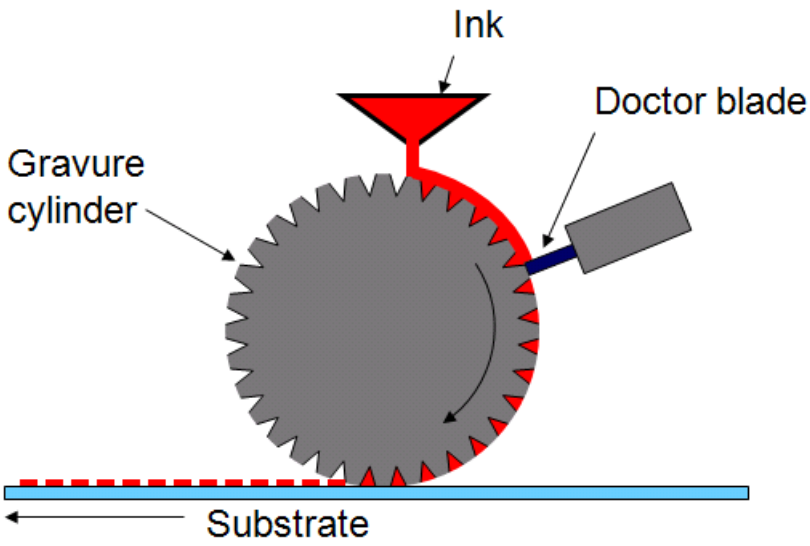

Figure 4. Schematic of Printing Process for Laboratory Gravure Printer [Source: Alejandro de la Fuente]

The laboratory printer uses sheetfed substrates instead of a continuous web, which results in each print run being limited to only three revolutions of the cylinder. Despite the short run length, there is a strong indication that the print is stabilized after only two revolutions, since the third revolution typically prints nearly identically to the second revolution. Each printed sample is approximately two feet long. One concern with the short run length is that it is difficult to print at extremely high speeds, because the linear motor takes time to accelerate the stage. For this reason, most experimental work is conducted at relatively slow print speeds.

As a consequence of the small printer size, the cylinder sizes are at the minimum limit of what is currently available. Figure 5 shows a blueprint of the laboratory gravure cylinder, which has a diameter of 2.62 inches and a face length of 2 inches. In contrast, a typical industrial cylinder ranges from 4-40 inches in diameter and 1-20 feet in face length.

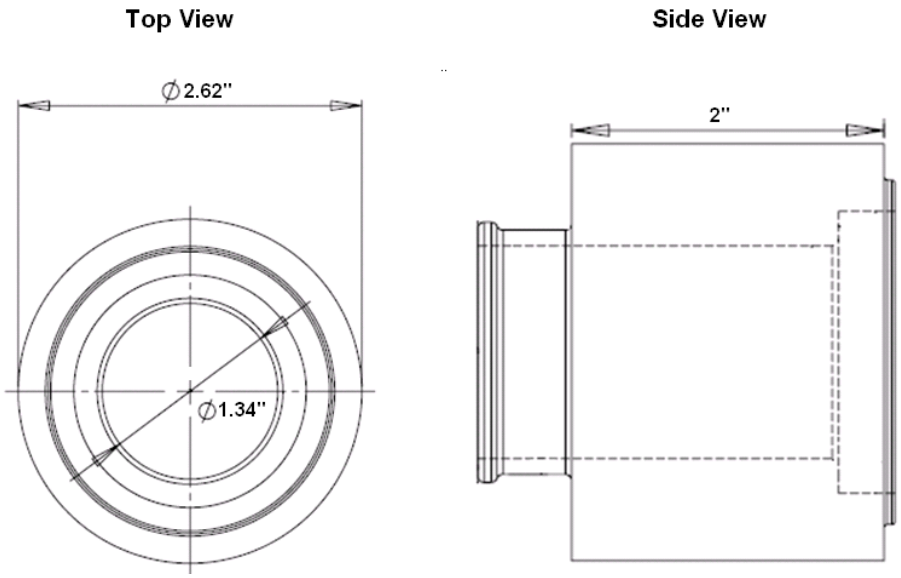

Figure 5. Blueprint of Gravure Cylinder [Source: Alejandro de la Fuente]

Although the laboratory rolls are small, the basic principles of printing remain the same, and the printing conditions are similar to those in industry. Thus, the printing trends discovered with this printer should be transferable to an industrial printer. The main challenge lies in identifying trends at high print speeds, since the typical industrial print speed of 5-10 m/s is clearly beyond the capabilities of the laboratory printer.

2.2 Techniques for Cylinder Making

This section will discuss techniques for optimizing the gravure cylinder, which is one of the most important elements of the printing process. Industrial best practices will be presented along with techniques discovered in the laboratory. The choice of cylinder material will be discussed, followed by an explanation of the different metrics for determining acceptable cylinders. Next, four methods of patterning cylinders will be compared.

The majority of industrial cylinders have a steel core with a copper surface covered by a thin layer of chrome. Figure 6 shows a top view of a typical copper/chrome cylinder and a process flow for producing cylinders. After a cylinder is taken off the press, it can be reused by stripping the chrome and copper. The press operator will then electroplate a new layer of copper, polish the copper, and pattern the surface. Afterwards, a thin layer

of chrome is deposited to protect the cylinder from wear. We chose to work with copper/chrome cylinders because copper and chrome are both well understood and most industrial machines are optimized to work with these materials.

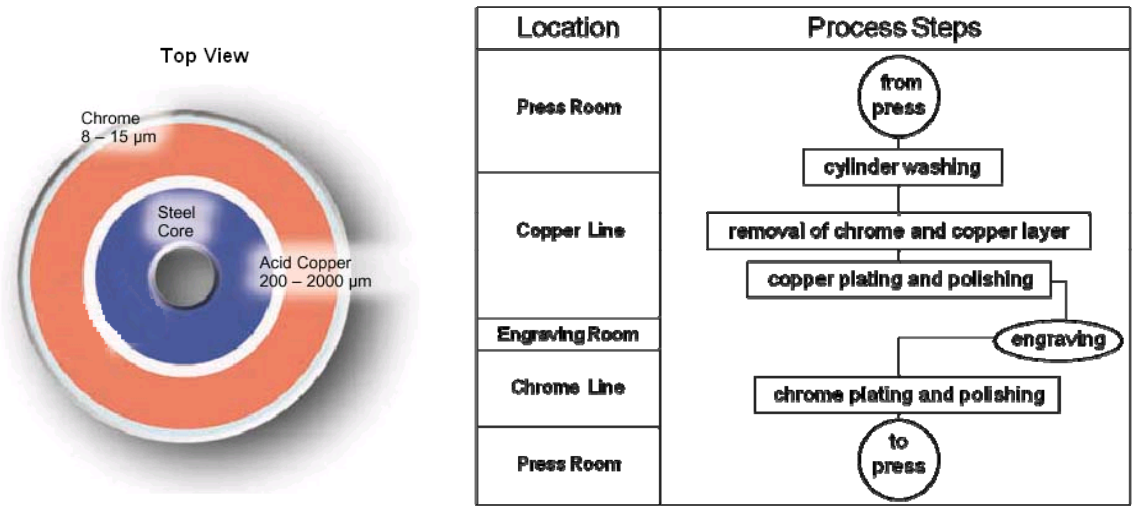

Figure 6. Top View of a Copper/Chrome Cylinder and Process Flow for Reusing Cylinders [GAA]

The surface material, copper, must fulfill the three basic functions of engravability, stability in the press, and reproducibility. Copper is a relatively soft material that can be easily engraved or etched with predictable results. It has the stability required to withstand the wiping pressure of the doctor blade during printing, such that ink is not transferred from the non-image areas of the cylinder and there is no “scum” on the print. Additionally, it can be polished and grinded to produce the appropriate surface finish. Grinders are used to level out large-scale unevenness in the cylinder, while polishers use a series of successively finer polishing stones to reduce the cylinder’s surface roughness.

In order to reduce wear on the blade and prevent scum, there are tight tolerances on the following cylinder metrics: Total Indicated Runout (TIR), taper, and surface roughness and waviness. The TIR is a measure of the concentricity of the cylinder face, and correlates strongly with the dynamic balance of the cylinder. The taper is the difference in diameter between the two faces of the cylinder, and should be less than 10 microns. Attempts to hand-polish cylinders using a lapping machine in the Cory Hall Machine

Shop were unsuccessful because of significant variations in the TIR and taper. The best polishing results have been obtained through the use of automated machines.

The surface roughness and waviness are measured in the copper, because any defects in the copper layer will be transferred to the chrome layer. The waviness measures large-scale unevenness and should be less than 1 micron over a measuring length of 15 mm. The surface roughness is a measure of the short-scale unevenness, and is commonly described by three metrics, which are shown in Figure 7.

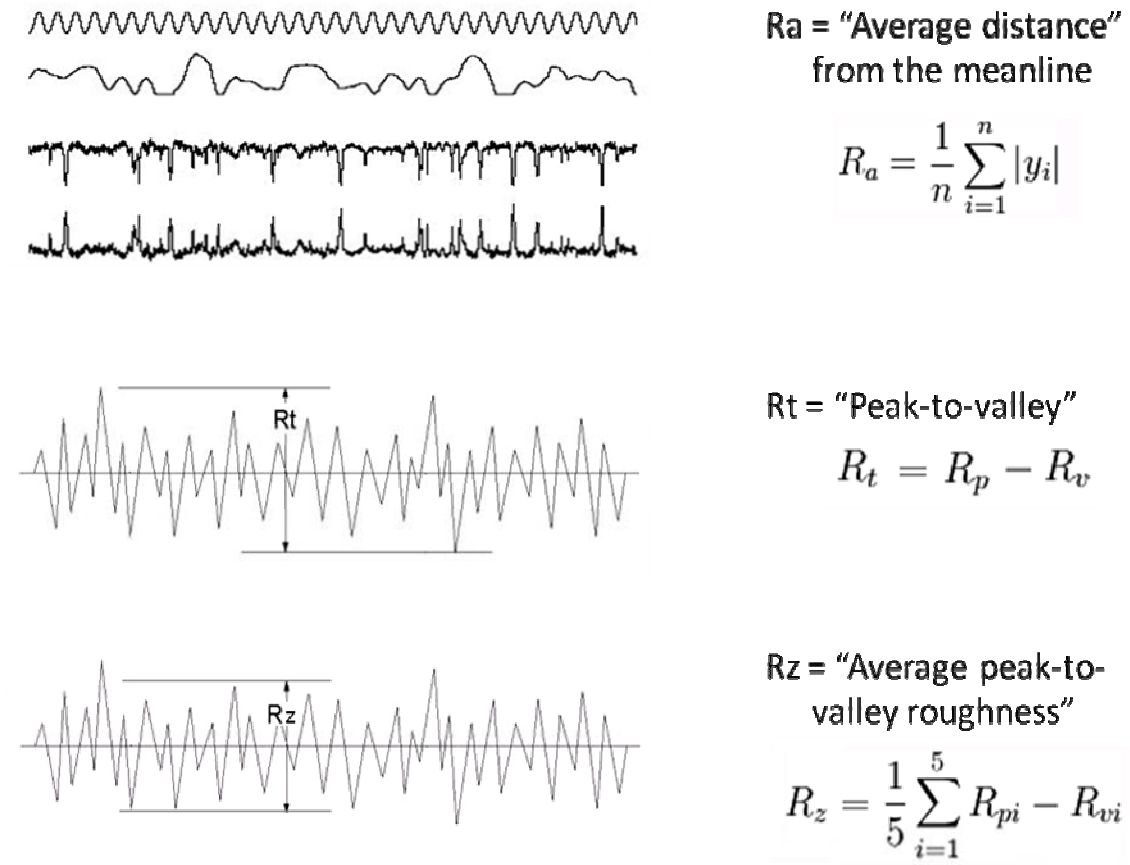

Figure 7. Surface Roughness Metrics *Ra, Rt,* and *Rz* [DMS]

Ra is the arithmetic average of the absolute values of the roughness profile from the meanline. It is commonly used in many non-gravure applications, but it has no value in identifying acceptable cylinders. As seen in Figure 7, different roughness profiles with different wiping characteristics can all have the same *Ra*. In contrast, *Rt* and *Rz* are peak-

to-valley measurements with much more discriminating value. It is always true that *Rt* >= *Rz* >= *Ra*.

As a measure of the average peak-to-valley roughness, *Rz* is the most commonly cited metric for identifying acceptable cylinders. One key element of a good cylinder is that its non-image areas are smooth enough to avoid transferring ink during the printing process. For most graphic arts applications, the typical *Rz* is 300-600 nm, as measured by a contact profilometer across a scan length of a few inches. However, for the purpose of wiping nanoparticle inks, the best *Rz* is around 200 nm.

The quality of the copper is extremely important in order to achieve the proper *Rz*. Copper quality is quantified by measuring the surface hardness, which is typically around 200 Vickers (HV). Attempts to polish a cylinder with low-quality copper resulted in a best-case *Rz* of around 710 nm. Additionally, experimental data indicate that the best printing results are obtained when the cylinder is cross-polished with the polish direction set at 45-60°. The cross-polish is essential to prevent scum, which will be discussed in more detail in a later section.

Preliminary experiments show that non-protected copper rolls can only withstand a few print runs before becoming unacceptably scratched. For this reason, the chrome layer is essential to increasing the lifetime of the cylinder. Typical chrome hardness is around 1,100 Vickers. The chrome is not only useful for reducing the friction from the doctor blade, but is also essential for lubrication between the doctor blade and cylinder surface during printing. The lubrication reduces wear on the cylinder and is aided by chrome microcracks created during the electroplating process. A recommended level of chrome cracks is 200-300 cracks per linear centimeter [GAA]. Figure 6 provides a close-up image of the best polished laboratory cylinder, contrasting cross polish marks and chrome cracks. The chrome cracks are extremely small compared to the cross polish marks, which can be up to four microns in length and one micron in depth.

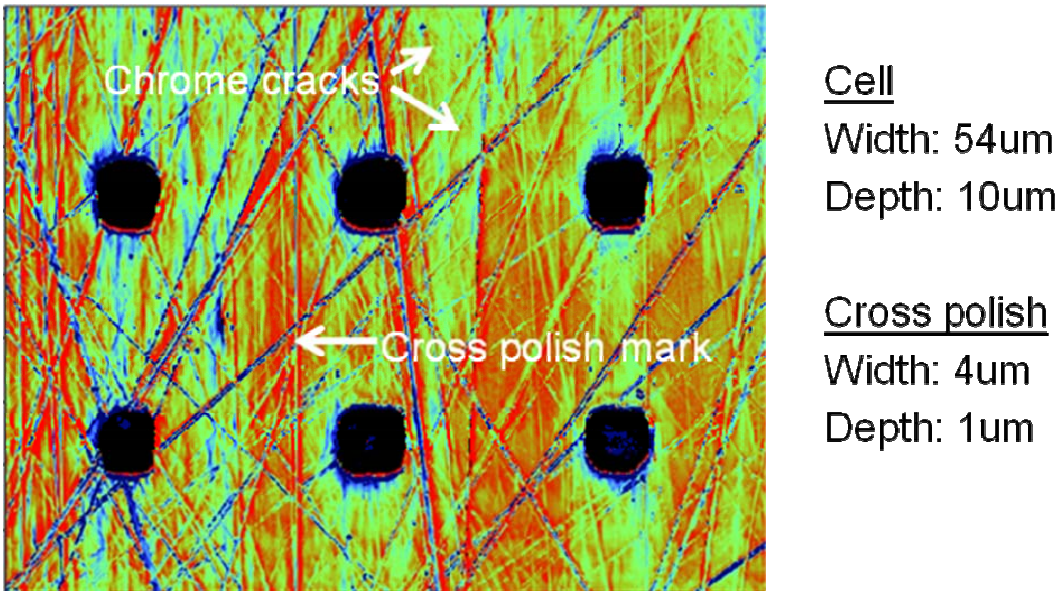

Figure 8. Close-up of Chrome Cracks in Polished Cylinder

The small laboratory cylinders also experienced a "rounding" of the edges, shown in Figure 9. This occurred because the diameter of the polishing stone was actually larger than the face length of the cylinder, which resulted in more pressure being applied to the edges of the cylinder. The rounding caused an imperfect contact with the doctor blade during printing, which occasionally resulted in ink leaking over the edges and ruining the final print. This will be an important issue to avoid as we scale to larger cylinders.

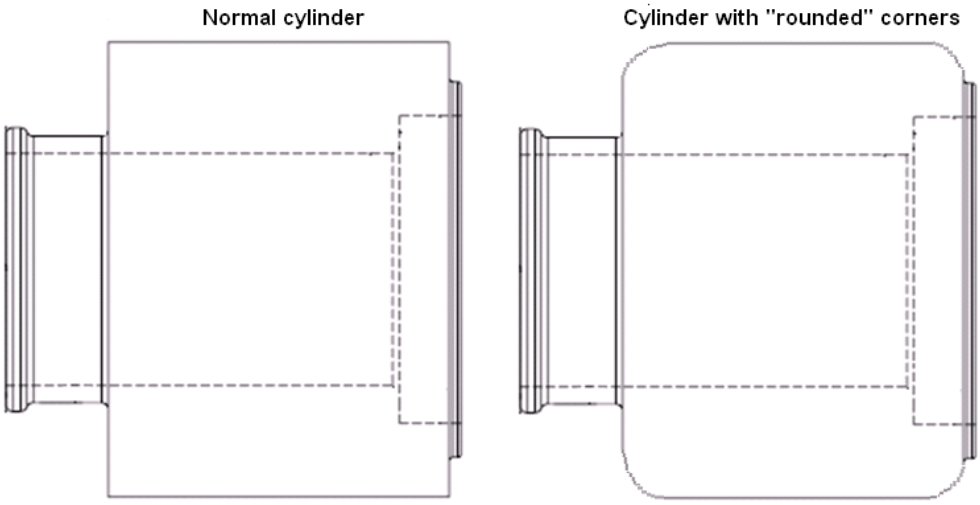

Figure 9. Cylinder with "Rounded" Corners [Source: Alejandro de la Fuente]

The four patterning methods considered for this project are electromechanical engraving, direct laser patterning, chemical etching, and indirect laser patterning. All four methods have the ability to transfer digital images directly to the cylinder surface, which allows for flexibility in the design process and shorter lead times. Digital files must be in a raster format, which uses a grid of pixels to represent images, as opposed to a vector format, which uses lines and curves. Raster images can easily be produced in standard graphics programs such as Adobe Photoshop.

In the graphic arts industry, images are screened according to the desired image sharpness and tonal variations, as well as ink and substrate parameters. Typical screens range from 50-500 lines per inch (LPI), which results in average cell widths of 30-350 microns. For typical graphic arts applications, the cell sizes must be kept to strict tolerances of a few microns over the entire cylinder surface, since even minute variations can cause undesirable defects visible to the naked eye. The cell uniformity requirements are even more stringent for printed electronics, because the final printed feature must be electrically functional and not simply visually pleasing. Both the cell size uniformity and the minimum achievable cell width must be improved in order to print uniform conductive lines less than 20 microns wide. The patterning requirements for this project are pushing the limits of what is currently possible in the industry.

The electromechanical method is the most consistent and commonly used engraving method. It uses a sharp diamond tip to cut copper out of the cylinder surface, producing diamond-shaped wells of varying width and depth. As shown in Figure 10, the spacing between adjacent cells remains constant for a given screen, but the width and depth can be varied by changing the indentation force. The cell aspect ratio is largely determined by the tip engraving angle, which is typically 110-140°. The aspect ratio can be tuned by changing the screen angle, which varies between 30-60°.

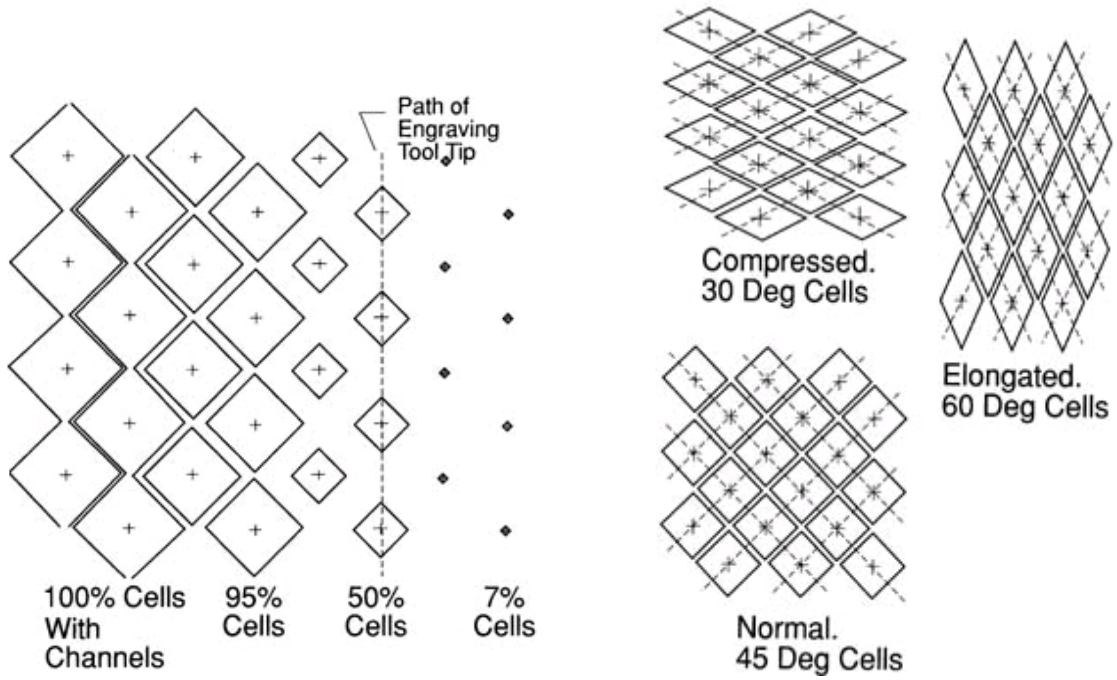

Figure 10. Cell Sizes and Screen Angles for Electromechanical Engraving [GAA]

Electromechanical engraving is a promising patterning technology for printed electronics. In theory, the screen can be set as tightly as desired, which would allow for the creation of cells with 5 micron widths and spacing. However, modern machines are not optimized for screens above 600 LPI, and there is a concern that small cells would not be able to carry enough ink, even if the engraving tip is changed to a sharper angle of 90-100°. Additionally, all cells are constrained to a diamond shape, which makes it difficult to place them close enough to print continuous lines. At this time, we cannot test the validity of these concerns, because the laboratory cylinders are too small to fit into industrial engraving machines. As we scale to larger cylinders, electromechanical engraving will remain a viable option.

The second considered method is the direct laser method, where the cylinder is patterned by a pulsating laser beam. The cell geometry is defined by the diameter and energy of the laser beam, which allows for a wide range of cell shapes and sizes. The minimum achievable cell width is currently about 20 microns, which is too large for printing sub-20-micron lines. Additionally, modern laser engraving systems are designed

to work with zinc-plated rolls instead of copper/chrome rolls. For these two reasons, the direct laser method is unsuitable for this project and will not be discussed further.

The chemical etching method is virtually identical to the photolithographic patterning process used in silicon microelectronics. Figure 11 is a schematic of a simple process flow that was developed in the UC Berkeley Microfabrication Laboratory (Microlab). The cylinder is first blade-coated with a thin layer of I-line photoresist, then covered with a flexible PET mask and exposed with a UV lamp. The roll is continuously rotated during the exposure to ensure uniform dosage. Next, the photoresist is developed and the cylinder is immersed in a beaker of ferric chloride (FeCl) etchant. Finally, the resist is stripped off the cylinder.

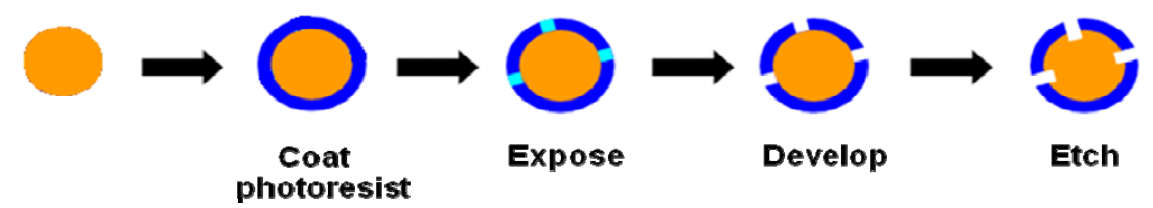

Figure 11. Process Flow for Chemically Etching Cylinders [Source: Alejandro de la Fuente]

The wet etch of the copper results in a significant amount of sidewall etching, which limits the achievable cell depth for a given width. The smallest features patterned with this method are about 12 microns in width but less than 1 micron in depth, which is much too shallow to print effectively. One way to minimize the sidewall etching is to spray the etchant onto the surface in fixed amounts instead of simply immersing the entire cylinder. Both the spray angle and the time between successive applications must be optimized. The best etching results have been achieved via an industrial etching process utilizing this spray technique. Figure 12 compares the aspect ratios of the Microlab etched roll to an industrially etched roll. For a cell width of 64-67 microns, the industrial roll achieved more than 10X increase in cell depth. For a cell width of 12 microns, the industrial roll achieved more than 5X increase in cell depth.

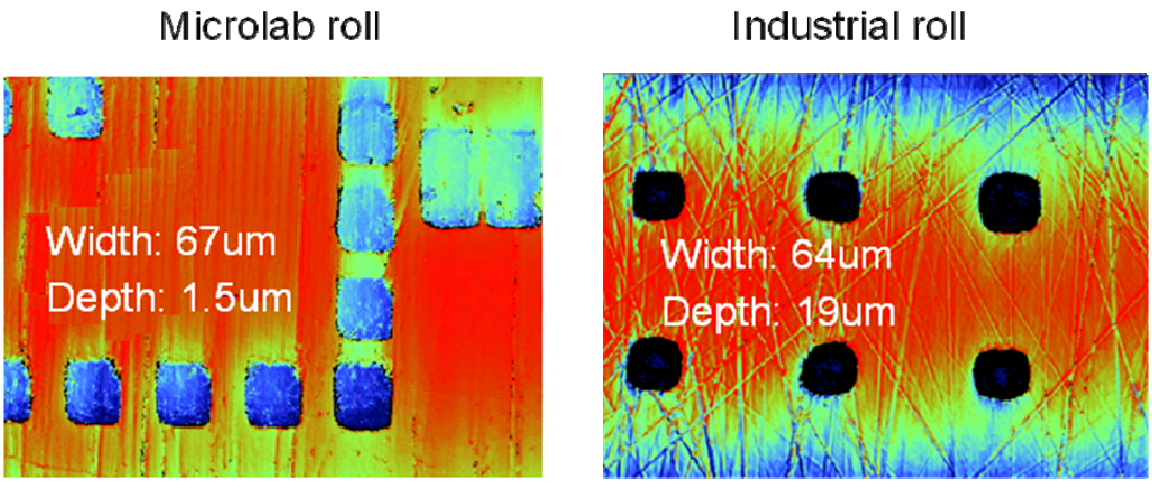

Figure 12. Comparison of Microlab Roll to Industrial Roll

Compared to the electromechanical method, the chemical etch method produces cells with greater volume. Chemically etched cells are semispherical or nearly cubic in shape, while electromechanically engraved cells are pyramidal in shape. The aspect ratio of chemically etched cells can be varied by changing the concentration and dose of the sprayed etchant, but it is difficult to significantly change the aspect ratio for cell widths below 40 microns. The main disadvantage with the chemical etch method is its relatively low uniformity and its inability to pattern small features consistently, due to nonuniformities from the exposure and develop steps.

The indirect laser method combines elements of both the direct laser and the chemical etch method. In this process, the photoresist is removed by laser, followed by a chemical etch of the cylinder. Preliminary tests show that this method tends to produce more uniform features than the chemical etching method, particularly for smaller feature sizes. Figure 13 compares etched cells for both methods. The cell widths were set at 10 microns in the digital file submitted to the engraver. On average, the indirect laser method produces cells which are smaller and more uniform. The chemically etched roll had cell widths ranging from 10-25 microns, while the indirectly laser patterned roll had cell widths ranging from 11-15 microns. The cell depth for both rolls was 4-5 microns.

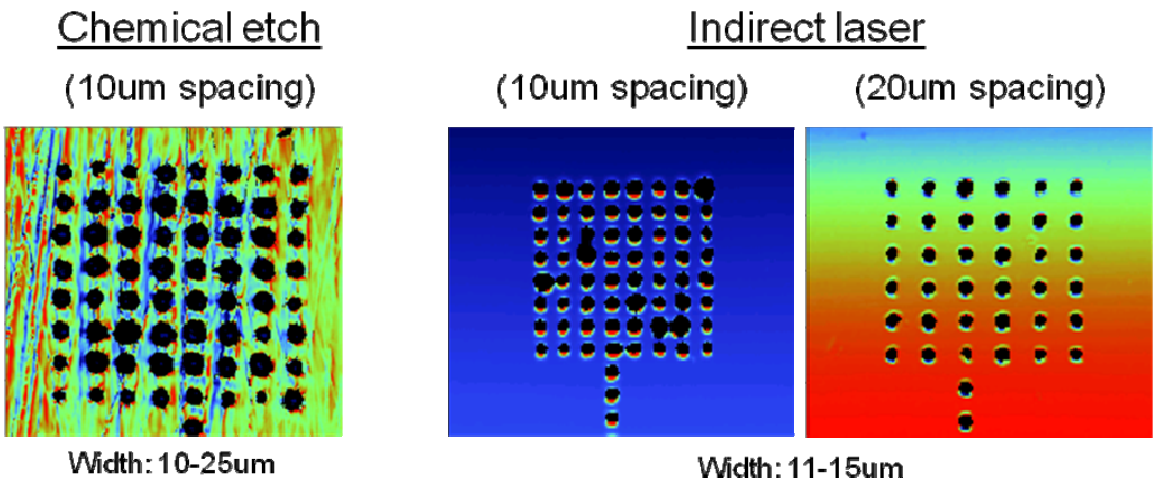

Figure 13. Comparison of Chemical Etching with Indirect Laser

The indirect laser method is more uniform than the chemical etch method because it avoids the exposure and developing steps, which removes two significant sources of nonuniformity. However, it still has uniformity problems resulting from loading effects during the wet etch step, especially at tighter cell spacing. As seen in Figure 13, the cells tend to be slightly wider at 10 micron spacing as compared to 20 micron spacing. Occasionally, these cells are so wide that they merge with neighboring cells and ruin the grid structure.

The cell uniformity will be especially important as we scale our etching techniques to larger cylinders. If we continue to use a sprayed wet etch, then the final cylinder size will probably be limited to at most a few feet in length because of etch nonuniformities across the length of the roll. One possible solution is to develop a dry etching process for the cylinder surface, which will involve developing a new plating and plasma etching technology. This approach is currently being investigated.

References

[DMS] Digital Metrology Solutions. http://www.digitalmetrology.com/Tutorials.htm

[GAA] Gravure Education Foundation and Gravure Association of America. *Gravure: Process and Technology*. Versailles, KY. 2003.

Chapter 3: Results and Optimization

3.1 Theoretical Considerations

This section will discuss the theoretical considerations necessary to develop a printing process to deposit conductive lines less than 20 microns wide, suitable for bottom-gate TFTs. We will first consider the characteristics of an ideal gate line. We then discuss the physical principles governing the gravure printing process, which can be separated into the two actions of cell emptying and drop spreading. We also discuss the conditions necessary for good wiping. Finally, we discuss a method to print conductive lines.

The ideal gate line is narrow, straight, and smooth. Narrow and straight lines allow for a smaller channel length and reduced overlap capacitance, which is essential for improving the performance of the TFT. The requirement of smoothness is especially important so that the dielectric layer above the gate can be as thin as possible, which will increase the gate capacitance. Smoothness is an important factor in determining suitable inks. We immediately ruled out the silver flake ink used in industrial RFID antennas, because it resulted in printed lines with unacceptably high surface roughness. We chose to use a silver nanoparticle ink to print the gate line, since our group has already demonstrated the viability of gold nanoparticles for inkjet-printed gate lines [Molesa].

The relationship between cell size and printed dot size is not a simple linear one, but it can be analyzed in terms of physical principles. A schematic of the gravure printing process is depicted in Figure 14. As a filled cell approaches the substrate, ink will be pulled out of the cell. The resultant drop will then spread on the substrate. The final width and thickness of the printed dot is highly dependent on the width and depth of the cell.

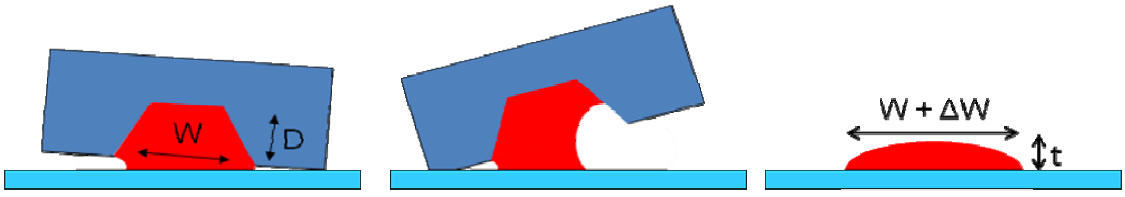

Figure 14. Schematic of the Gravure Printing Process: (a) Cell Emptying (b) Drop Spreading [Source: Alejandro de la Fuente]

The printing process can be divided into the two basic actions of cell emptying and drop spreading. The cell emptying is affected by a number of variables, including the cell width, cell aspect ratio, print speed, ink viscosity, and substrate surface energy. Cells with smaller widths and larger aspect ratios tend to print less ink because they have a larger surface area to volume ratio, which results in greater adhesive forces which keep the ink in the cell [Yin]. In contrast, substrates with high surface energy will tend to pull the ink out of the cell. The print speed is important in determining the shear applied to the ink in the cell, while the ink viscosity determines its resistance to that shear. Higher viscosity inks have greater resistance to shear and tend to empty less completely than low viscosity inks.

After the drop leaves the cell, it will attempt to minimize its interfacial surface energy by spreading on the substrate. If the drop has a low surface tension relative to the substrate surface energy, then it will tend to spread more, since the larger interface will lower the overall surface energy. Thus, the printed dot size can be minimized by either increasing the ink surface tension or decreasing the substrate surface energy [Liang]. Figure 15 shows three fluids with different surface tensions. *A* shows a fluid with high surface tension and little wetting, while *C* shows a fluid with low surface tension and more wetting.

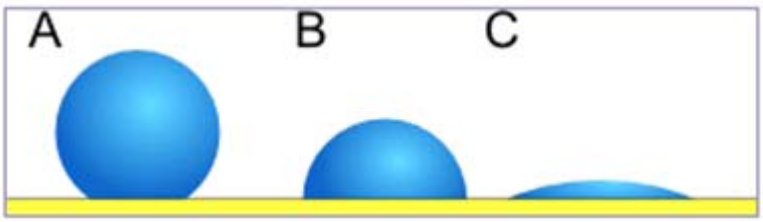

Figure 15. Drop Wetting of Different Fluids.

In addition to ink surface tension, the ink viscosity also plays a role in the spreading process, because it determines the ink's internal resistance to flow, and a low ink viscosity can cause a print to “bleed out” and reduce image sharpness [GAA]. The most carefully monitored ink parameter in the industry is the ink viscosity, not the surface tension. The viscosity is much easier to measure than the surface tension, and the two

parameters tend to be correlated in many inks. Ink viscosity is commonly measured with a Zahn cup, which is a stainless steel cup with a tiny hole in the bottom of the cup. To measure the viscosity, the user measures the amount of time it takes for ink to empty a completely filled Zahn cup, also known as the "efflux time." The efflux time is 16-24 seconds for most color inks, which corresponds to a typically quoted viscosity of 10-25 centipoise (cps). However, it is important to note that most inks are non-Newtonian fluids and the viscosity is highly dependent on the shear rate.

Figure 16 compares the viscosity profile of a purple-colored ink used in graphics applications to the viscosity profiles of various dilutions of a silver nanoparticle paste sold by Advanced Nano Products [ANP]. The purple ink is a water-based ink with an efflux time of 20-22 seconds, while the undiluted silver nanoparticle paste is a solvent-based mixture with a given viscosity of 5,000-20,000 cps. To create the various dilutions, we mixed the paste with different amounts of alpha-terpineol by % volume. Thus, the "ANP 50%" dilution is 50% paste and 50% alpha-terpineol by volume. All viscosity measurements are made with a Brookfield DV-III Cone/Plate Viscometer.

.

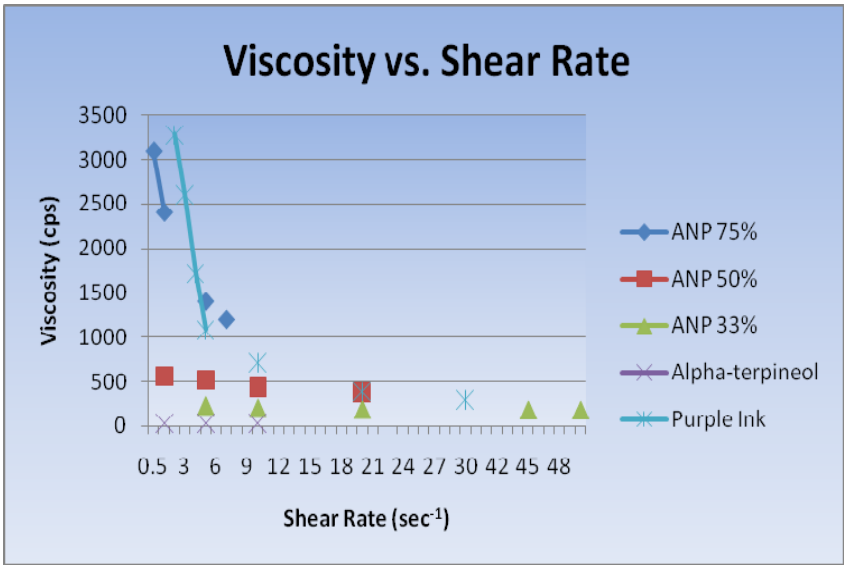

Figure 16. Viscosity vs. Shear Rate for ANP Silver Nanoparticle Ink.

As expected, all the inks are shear-thinning. It is important to note that the shear rates in the above graph are several orders of magnitude smaller than the shear rate that is actually applied from the doctor blade during printing. Assuming simple shear, the shear

rate during printing is equal to the print speed divided by the height of the fluid film between the blade and cylinder as the wiping occurs. With a print speed of 0.1 m/s and film height of around 5 nm, a quick calculation shows that the shear rate is around 5E7 sec^{-1}. This means that the effective viscosities of the inks are most likely lower than the viscosities shown in the graph.

The effective viscosity of the ink plays an important role not only in cell emptying, but also in the wiping action of the doctor blade during printing. Wiping is primarily a mechanical action and does not depend strongly on surface tension effects. Figure 17 shows a diagram depicting the interaction of the doctor blade with the cylinder surface. The footprint of the blade determines the area of interaction with the cylinder surface, and should be kept constant over the lifetime of the blade. It is thermodynamically impossible to achieve a completely clean wipe purely through mechanical means, so there will always be a thin film of height *h* on the cylinder surface. This film is essential for lubrication, which is essential for good wiping and reduced wear of the surface. However, if the film thickness exceeds a certain threshold, then scum will appear on the final print. The film thickness *h* is dependent on a number of factors including the viscosity of the ink, the print speed, the blade angle and the cylinder surface roughness [Sullivan].

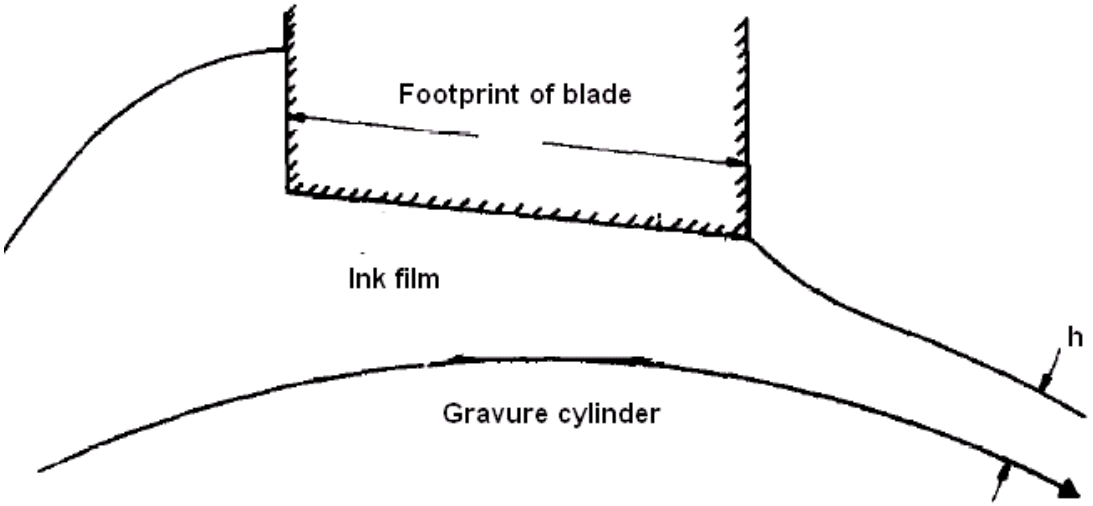

Figure 17. Interaction of the Doctor Blade with Cylinder Surface During Wiping [Sullivan]

For optimal wiping of nanoparticles, the cylinder must be cross-polished with an *Rz* of 200 nm. The cross polish marks fill with ink during wiping, but do not print onto the substrate because of their high aspect ratio and random orientation. If there is no cross-polish, then the cylinder is likely to print scum, regardless of the *Rz*. Using single point diamond-turning, we created a cylinder which had an *Rz* better than 200 nm, but which had continuous feed marks along the direction of print. These feed marks were only a few microns wide and less than half a micron deep, but they still ended up printing very thin scum lines because they extended around the entire cylinder and were not randomized like the cross polish marks.

Next, we discuss how individual drops can be placed closely together to form conductive lines. We consider the work of Soltman, who optimized printed gate lines by varying the spacing between drops of inkjet-printed PEDOT:PSS [Soltman]. There are three regimes of printed line behavior, shown in Figure 18. In image (a), the drops are spread far enough to form discrete dots. In image (b), the dots only partially intersect each other, resulting in "scalloped" lines which are slightly narrower than the individual drop width. In image (c), the drops form a smooth, continuous line. This occurs when the ratio of drop spacing to landed drop radius is 1.10, where the drop spacing is defined as the distance between the centers of neighboring drops.

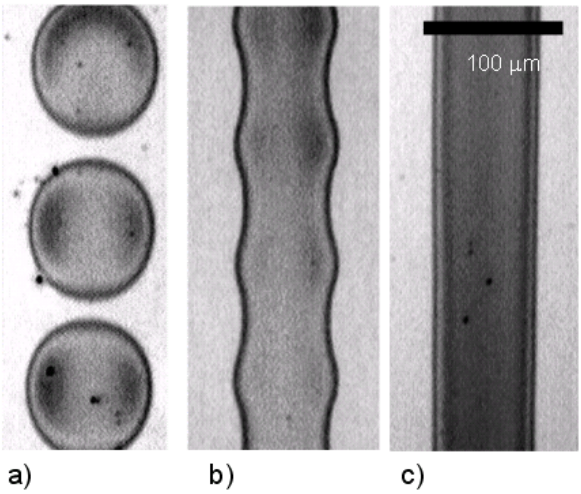

Figure 18. Examples of Printed Line Behaviors with Varying Spacing"
(a) Discrete dots (b) "Scalloped" line (c) Uniform line [Soltman]

In addition to the cell spacing, the ink viscosity must also be optimized to print uniform lines. If the ink is too viscous, then the drops will not flow into each other and the resultant line will have width and thickness nonuniformities. At the same time, the ink viscosity cannot be too low, or the printed line will be too thin. It is important to maximize the printed line thickness, because thicker lines tend to have more uniform print heights [Smits]. The viscosity of the PEDOT:PSS is 121 cps at a low shear rate of 1.9 sec^{-1}, while the viscosities used in this project vary from 250 to 2400 cps at the same shear rate.

3.2 Experimental Outline

In this section, we will review the printing conditions that were used and then describe the experimental outline. We first discuss the choice of doctor blade. The two types of blade tips that are commonly used are bevel and lamella, as shown in Figure 19. The bevel blade has a tip angle of either 2° or 15°, and is designed to provide a very clean wipe. The lamella blade is used for longer runs, and is designed to maintain a uniform contact area width even as it wears with use. We chose to use a 2° bevel blade in our printing process, since our print runs are short and the bevel blade has a sharper edge which seems to wipe nanoparticles more effectively than the lamella blade. The doctor blade was set at a standard contact angle of around 60° with a blade pressure of 40 psi.

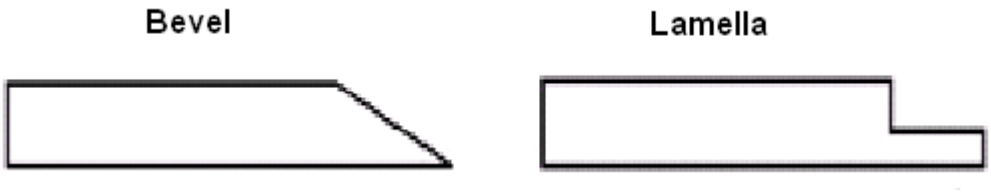

Figure 19. Bevel and Lamella Doctor Blades

Next, we discuss the print speed. At high print speeds, the transfer of ink to substrate is greatly reduced, and most industrial printers must use a technique called electrostatic assist (ESA) to improve cell emptying. Our laboratory printer lacks the ESA function, so we chose to print at a relatively slow speed of 0.1 m/s in order to ensure that we had a completely stable printing process.

We now turn to the experimental outline. The independent variables in this experiment are cell width, cell depth, cell spacing, and viscosity. In order to test the effect of these variables on print quality, we mixed four different dilutions of the ANP silver nanoparticle ink by % volume and patterned two test cylinders with the chemical etch and laser ablation methods. Figure 20 shows the three different cell configurations on the cylinders: individual dots, gravure lines, and intaglio trenches. There are a wide range of cell widths and cell depths, with the widths ranging from 10 to 64 microns and the depths ranging from 4 to 19 microns.

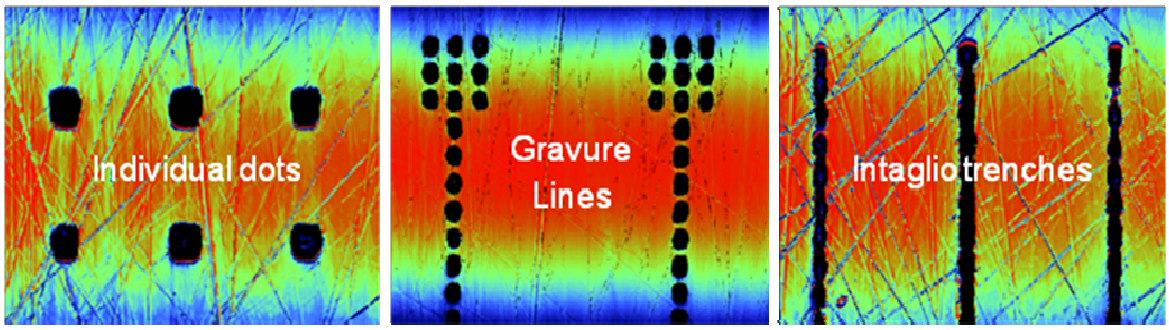

Figure 20. Three Different Cell Configurations on Test Cylinders:
(a) Individual Dots (b) Gravure Lines (c) Intaglio Trenches

The dependent variables in this experiment are printed line width and printed line thickness. It is important to note that the line thickness is measured only after annealing each sample at 150°C for 30 minutes. Many of the printed lines have variations in width and thickness due to non-optimal spacing of cells and nonuniformities in cell size. We smooth out these variations by averaging the width and thickness over a 500 micron-wide cross-section for each line. Measurements are made with the Wyko NT3300 Profiling System, which is described in more detail in Appendix A.

3.3 Effect of Viscosity and Cell Parameters on Print Quality

The experimental goal of this project is to develop a printing process to deposit conductive lines less than 20 microns wide, suitable for bottom gate structures. In this section, we demonstrate gravure-printed nanoparticle lines and present techniques for optimizing the printed line quality by varying print parameters such as cell spacing and

viscosity. We will first examine the printing behavior of individual drops and identify an optimal ink dilution. We then examine the behavior of printed lines resulting from closely spaced dots, and discuss the minimum width printed line. Finally, we investigate intaglio trenches as an alternate method for printing conductive lines.

Individual dots

When printing individual dots, the cell aspect ratio must not be too low, or the cylinder will print "donuts," which are printed dots with an empty space in the middle. Figure 21 shows a comparison of prints between the Microlab and industrially etched roll, which have very different cell aspect ratios. The Microlab roll prints donuts because its cells are too shallow and there is not enough ink in each cell to print a complete dot. Experimental data shows that the cell width over cell depth ratio must be smaller than 7-8 in order to avoid donuts.

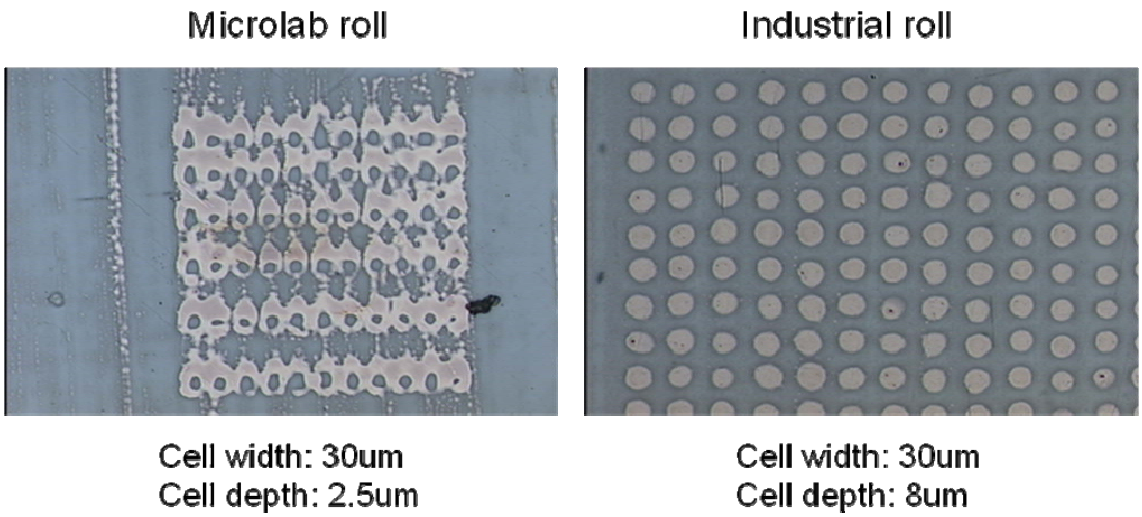

Figure 21. Comparison of Prints from Rolls with Different Cell Aspect Ratios (ANP 50%)

Figure 22 is a set of graphs depicting the relationships between cell width and cell depth with printed dot width and thickness. Figures 22a and 22d show the correlation between cell width and cell depth for four different patterns, labeled 'PAT #a' to 'PAT #d.' The chemical etch method was used for 'PAT #a' to 'PAT #c,' while the indirect laser method was used for 'PAT #d,' since the chemical etch method was unable to

consistently pattern features smaller than 20 microns in width. As mentioned in section 2.2, the minimum-sized cells were 11-15 microns in width, with an average width of 12 microns. The fifth method, 'IGT,' refers to an electromechanically engraved test roll created by IGT Testing Systems.

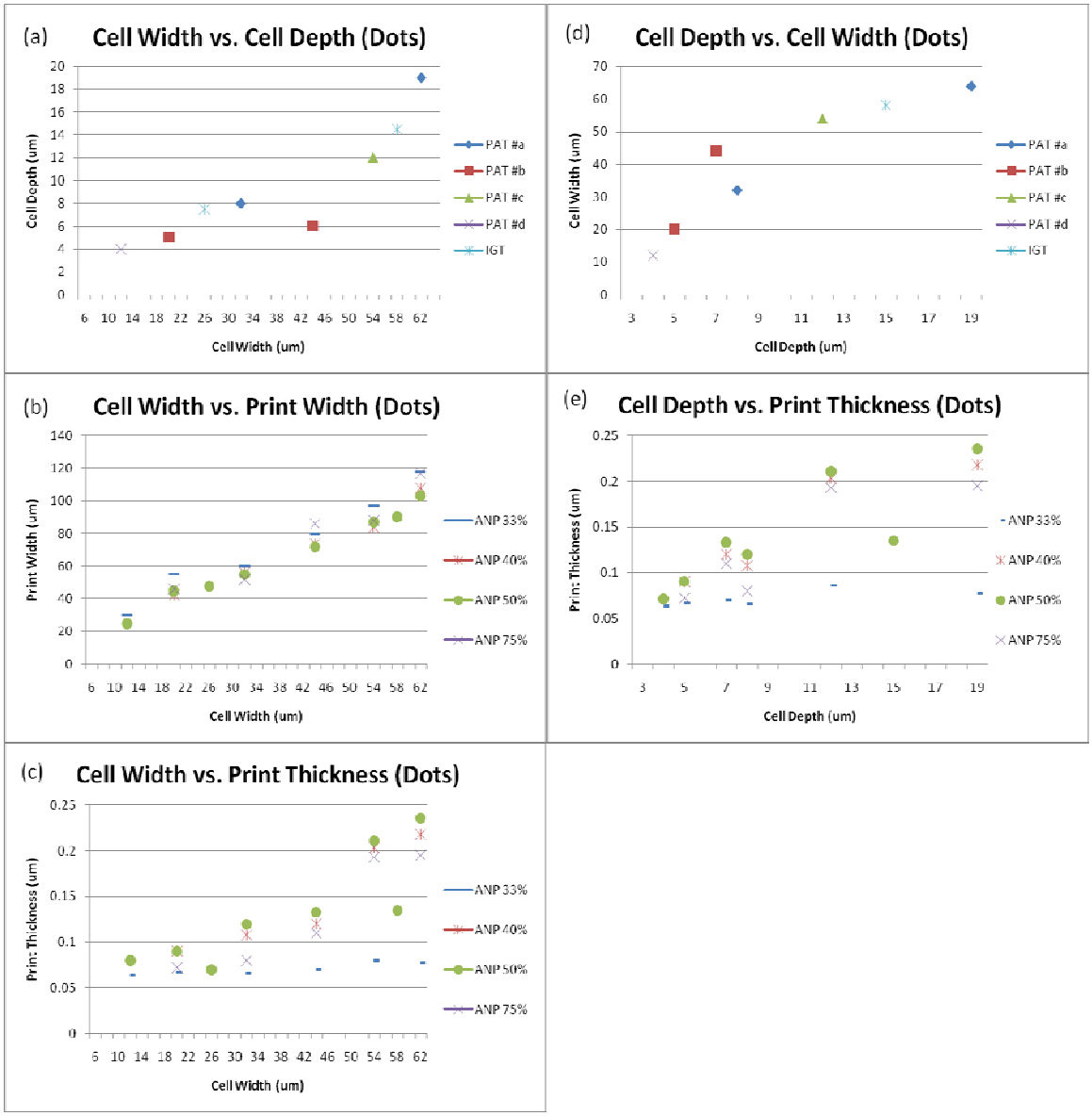

Figure 22. Relationship of Cell Width/Depth to Print Width/Thickness (Dots)

All the printed dot widths cited in Figure 22 are measured in the horizontal direction, since dots tend to spread more in the vertical direction of print. This vertical spreading effect is primarily seen in cells that are wider than 50 microns. Figure 22b shows that the

print width is linearly dependent on the cell width, irrespective of the cell depth. The lowest viscosity dilution, ANP 33%, consistently prints the widest dots, while the ANP 40% and ANP 50% dilutions print dots of essentially the same width. These results are not too surprising, since the ANP 40% and ANP 50% have the same contact angle with the PET substrate (19°), while the ANP 33% has a lower contact angle (10°). As explained in section 3.1, the drop spreading is primarily determined by the ink surface tension, not the ink viscosity.

The ANP 75% dilution has a higher contact angle than the ANP 50% dilution, and for the most part prints dots that have equal or smaller width. However, there are two cell widths for which the ANP 75% dilution actually prints a wider dot than the ANP 50% dilution. We can explain these two cases by examining the cell emptying. As mentioned in section 3.1, higher viscosity inks tend to empty less than lower viscosity inks. However, the cell may have unique characteristics that can mitigate this effect and enhance the amount of deposited ink, such that the final amount of silver left after annealing will be greater or equal for the higher viscosity ink. For these two cell widths, the cell characteristics that increase cell emptying are low cell aspect ratio in the case of the 44 micron wide cell and greater cell depth in the case of the 62 micron wide cell.

In contrast to the lower viscosity dilutions, the ANP 75% dilution tends to empty very inconsistently, and seems to be on the threshold of two printing regimes, as shown in Figure 2. Image (a) shows a normal printed dot, which occurs about half the time, while images (b) and (c) show partially printed dots. The half-moon shape in image (b) is commonly seen when printing high viscosity inks, because the cell emptying is so low that there is not enough ink leaving the cell to print a full dot.

(a) 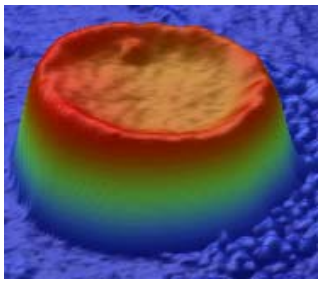 (b) 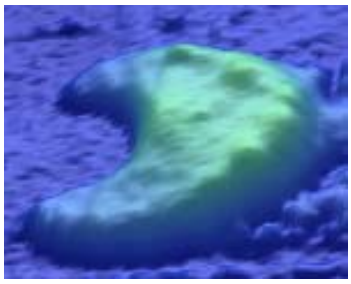 (c) 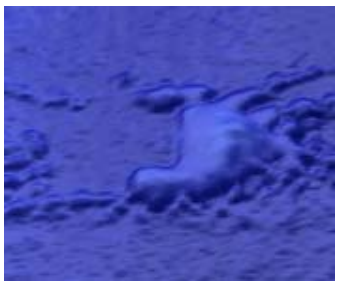

Figure 23. Three Different Instances of ANP 75% Dots

A satisfactory explanation for the inconsistent printing of the ANP 75% dilution has not been found, but it likely has to do with the effective ink viscosity varying along the length of the roll due to minute variations in blade pressure. For low viscosity inks with relatively constant viscosity profiles, these viscosity variations do not significantly change the cell emptying, but for relatively high viscosity inks like the ANP 75%, it seems that these variations are important. The ANP 75% empties from 20 micron wide cells only about 10% of the time, and does not print at all from 12 micron wide cells.

The minimum printed dot width was 25 microns, which was achieved by printing the ANP 50% dilution from 12 micron wide cells. It is important to note that this width is only an average value obtained from multiple dots. From the linear trend in Figure 22b, it can be clearly seen that scaling the minimum cell width to 5 microns would result in realizing the stated goal of printed conductors less than 20 microns wide. From the trend in Figure 22c, the print height for a 20 micron wide dot would be around 50 nm, which is more than adequate for a printed gate line.

Although viscosity has only a secondary effect on the printed dot width, it has a significant effect on the printed dot thickness, as shown in Figures 22c and 22e. In general, higher viscosities result in thicker dots, unless the viscosity is too high and the cell cannot empty properly. The ANP 50% dilution consistently prints the thickest dots, followed by the ANP 40%, ANP 75%, and the ANP 33% dilutions. There is a very strong correlation between the cell depth and printed dot thickness, but the correlation is not completely linear because wider cells also tend to print thicker dots. This contrasts with the strictly linear relationship between cell width and printed dot width, irrespective of cell depth.

By comparing the IGT cells to the other cells, we find that electromechanically engraved cells release much less ink than chemically etched cells. The IGT prints follow the same linear relationship between cell width and printed dot width, but they are also much thinner. This result is not too surprising since the cell volume for a given cell width is much lower for an IGT cell than for a chemically etched cell. This highlights an earlier concern that an electromechanically engraved 5 micron wide cell would not hold enough ink to print a complete dot. Figure 22c shows that a 26 micron wide IGT cell results in a printed dot thickness of 70 nm. If this were scaled to a 5 micron wide cell, the printed dot

thickness would likely be only 20-30 nm, which is probably too thin for a printed gate line.

From the above analysis, it is clear that the ANP 50% dilution is the optimal ink dilution because it consistently prints the narrowest, thickest dots across a wide range of cell widths and depths. We will pay special attention to this ink as we examine the behavior of printed lines resulting from closely spaced dots.

Gravure lines

Figure 24 is a set of graphs depicting the relationship between cell width, cell depth, and cell spacing with printed line width and thickness. Figures 24a and 24d show the correlation between cell width and cell depth. These two figures were originally intended to be identical to Figures 23a and 23d, but many of the cell widths changed because of loading effects during the wet etch. Each of these cells is set at 3 different cell spacings. Typically only one spacing prints a uniform line, while the other two spacings result in either scalloped lines or individual dots. This has important repercussions for our analysis of printed lines. As explained in section 3.1, printed lines are the most uniform and narrow when the dimensionless radius, or ratio of drop spacing to printed drop radius, is set to 1.10. If the dimensionless spacing is slightly greater or less than 1.1, the printed lines will not be optimized, but they will still be fairly uniform. This is the case for all the lines in Figure 24.

Figure 24b shows the relationship between cell width and printed line width. The trends here are essentially identical to the trends discovered with printed dots, with two exceptions. First, the relationship is no longer completely linear, but instead is also dependent on the cell depth. Deeper cells tend to produce wider lines. Second, the ANP 75% dilution occasionally prints narrower lines than the other dilutions, as opposed to printing the lines of equal or greater width. This phenomenon is most likely explained by the fact that the ANP 75% dilution has an inconsistent print quality, which results in a significant number of cells printing only partial dots. Thus, a line printed with this dilution would tend to have gaps and significant nonuniformities, which will lower the overall width of the line.

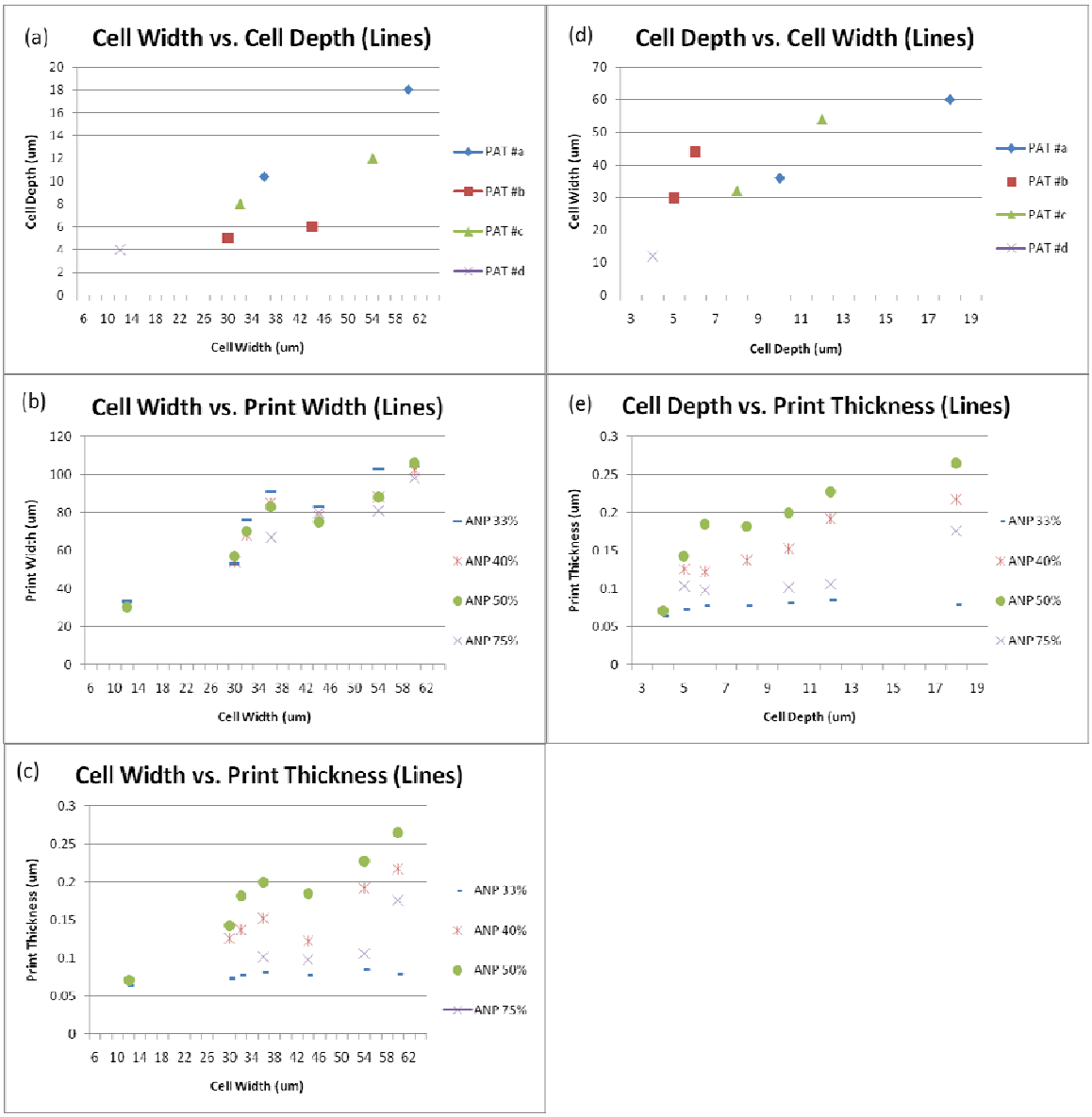

Figure 24. Relationship of Cell Width/Depth to Print Width/Thickness (Lines)

Figures 24c and 24e show the relationship between cell depth and printed line thickness. Again, the trends are essentially identical to the trends discovered with printed dots. As before, there is a strong correlation between cell depth and printed line thickness, but now there is also a dependence on the cell width. Once again, the ANP 50% dilution prints the thickest lines, followed by the ANP 40%, 75%, and 33% dilutions. There is virtually no change in the print height with the ANP 33% dilution.

Figure 25 compares the three-dimensional morphology of lines printed with 3 different dilutions. These lines are printed from the largest available cells on the roll, which are 60

microns in width. The spacing between cell edges is 18 microns, and the dimensionless spacing is about 0.7. The line printed with the ANP 75% dilution is the narrowest line, but is also the most nonuniform in width and thickness. This is primarily related to its inconsistent print quality, but is also partly related to the fact that the ink is much more viscous and does not flow as easily. In contrast, the ANP 50% and ANP 33% dilutions have good print quality and low enough viscosity that they have good flow between printed dots, resulting in fairly uniform printed lines.

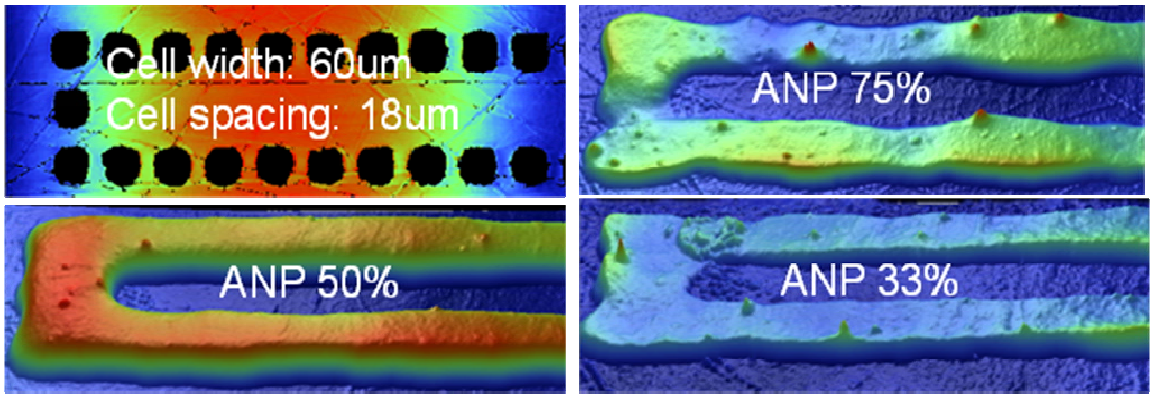

Figure 25. Comparison of Etched Cells with Printed Gravure Lines

Figure 26 shows the effect of cell spacing on the printed line width and thickness. For four different cells, we found two different spacings that both resulted in fairly uniform prints. The primary takeaway from these two graphs is that tighter cell spacing results in wider and thicker prints. This reinforces the point made earlier that if the drops overlap too much, the line will still be fairly uniform, but will not be as narrow as possible.

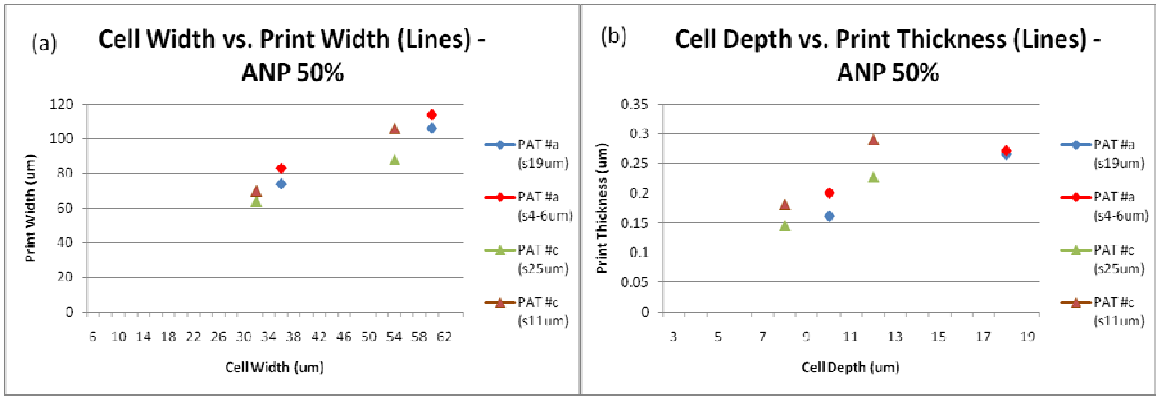

Figure 26. Relationship of Cell Width/Depth to Print Width/Thickness (Lines)

In order to print uniform lines, the cell spacing must be optimized such that the dimensionless radius of the printed dots is set as close to 1.10 as possible. This is especially important for cells smaller than 20 microns, since small variations of just 2-3 microns can have a significant impact on the dimensionless radius. Currently, the smallest available cells range from 11-15 microns wide, and the minimum printed line achieved is 30 microns width and 70nm thick. This line, shown in Figure 27, is currently not suitable as a gate line, because it has width and height nonuniformities resulting from variations in the etched cell size. Additionally, it was printed with an indirectly laser patterned roll without a proper cross polish, which resulted in scum on the print.

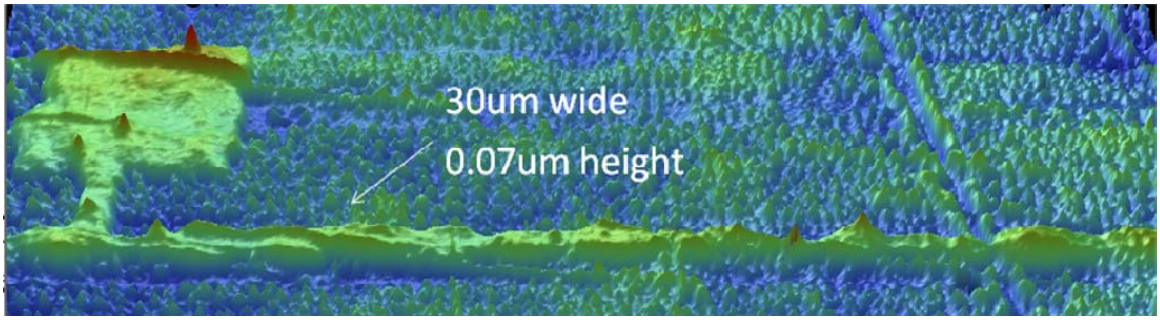

Figure 27. Minimum Width Printed Line

Intaglio trenches

Next, we investigate intaglio trenches as an alternate method for printing conductive lines. At first glance, intaglio trenches seem like a logical choice for printing conductive lines. First, they can be used to print lines without having to worry about optimizing the drop spacing and drop radius. Second, they can theoretically be scaled down to very small cell widths without having to worry about cell emptying, because the cell volume for a given cell width remains high.

Intaglio trenches have one important printing defect, however. Intaglio trenches that are parallel to the direction of print often exhibit a “pickout” effect, where a section of the printed line simply never transfers to the substrate, as shown in Figure 28. Pickout does not occur in horizontal trenches, and seems to be caused by fluid flow within the trench. It is not as easily explained as donuts, because the same trench will exhibit different amounts of pickout across multiple prints. One possible explanation of pickout

is that the doctor blade pulls out ink as it passes over the trench, and the inconsistency can be explained by slight variations in blade pressure across multiple prints. The amount of pickout appears to be somewhat random. It is not correlated to the cell depth, cell width, or viscosity.

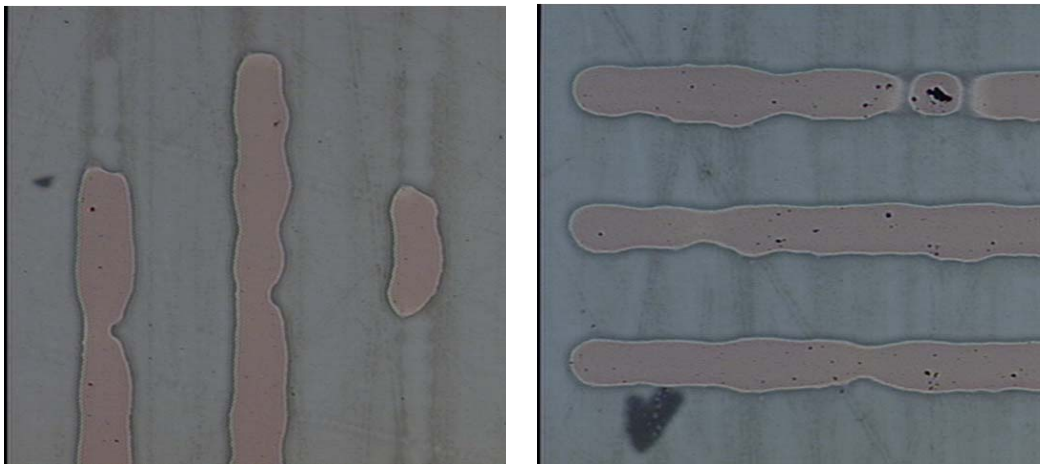

Figure 28. Pickout in Intaglio Trenches

Figure 29 is a set of graphs depicting the relationship between cell width and cell depth with printed line width and thickness for intaglio trenches. These measurements are given only for printed lines that do not have any pickout. Figures 29a and 29d show the correlation between cell width and cell depth. Figure 29b shows that the print width is linearly dependent on the cell width, with a slight dependence on cell depth. Similarly, Figure 29e shows that the print thickness is linearly dependent on the cell depth, with a slight dependence on cell width. These trends are essentially identical to the trends from printing gravure lines.

Overall, intaglio trenches have a number of disadvantages. First, they cannot be used when oriented along the direction of the print because of the pickout effect. Second, they tend to have greater variation in print width uniformity as compared to gravure lines, because of ink flow in the trench during transfer to the substrate. Third, intaglio trenches always print lines that are much wider than those printed from gravure lines. Fourth, the printed line width decreases only slightly as the cell width is decreased. From the trend in Figure 29b, it is clear that intaglio trenches could not be scaled to a small enough cell width to print a sub-20 micron line.

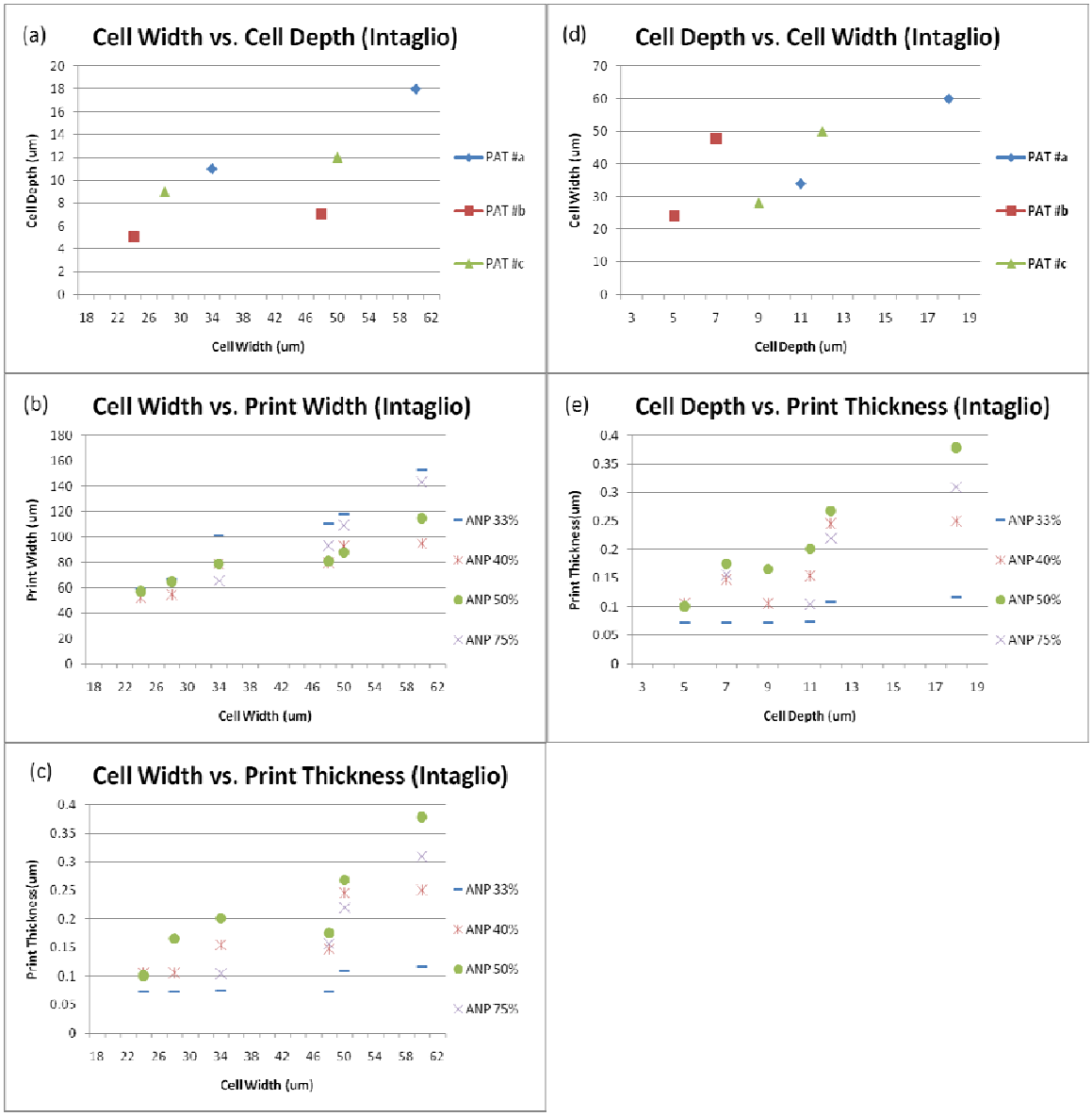

Figure 29. Relationship of Cell Width/Depth to Print Width/Thickness (Intaglio Trenches)

In this section, we presented a roadmap to achieve sub-20 micron lines. We identified an optimal silver nanoparticle dilution, and considered two different methods of printing conductive lines. We determined that the best method of printing uniform and narrow lines is to use individual cells with the appropriate spacing, such that the dimensionless radius is 1.10. We also identified several trends that can provide a direction for scaling to

smaller printed features. Currently, 30 microns is the minimum printed line width. At present, these lines are not suitable for bottom gate TFTs. In order to achieve conductive gate lines less than 20 microns wide, there are two main areas that must be optimized. First, the patterning uniformity must be improved, such that the cell size variance is less than a micron. Second, the minimum cell size must be scaled to at least 5 microns or below.

References

[ANP] Advanced Nano Products. http://anapro.com/english/product/product7.asp

[GAA] Gravure Education Foundation and Gravure Association of America. *Gravure: Process and Technology*. Versailles, KY. 2003.

[Liang] Liang, T.X. 1996 "Effect of Surface Energies on Screen Printing Resolution." *IEEE Transactions on Components, Packaging, and Manufacturing Technology*, Part B, Vol. 19, No. 2, 423-426.

[Molesa] Molesa, S., S. Volkman, D. Redinger, A. Vornbrock, and V. Subramanian. 2004. "A high-performance all-inkjetted organic transistor technology." *Technical Digest – International Electron Devices Meeting*, pp. 1072-1074.

[Smits] Smits, A.J. *A Physical Introduction to Fluid Mechanics.* Wiley. 1999

[Soltman] Soltman, D. and V. Subramanian. "Inkjet-Printed Line Morphologies and Temperature Control of the Coffee Ring Effect." *Langmuir*, 2008, **24** (5), 2224-2231.

[Sullivan] Sullivan, T. and S. Middleman. "Film thickness in blade coating of viscous and viscoelastic liquids." *Journal of Non-Newtonian Fluid Mechanics,* 1986, 21, 13-38.

[Yin] Yin, X. and S. Kumar. 2005. "Flow visualization of the liquid-emptying process in scaled-up gravure grooves and cells." *Chemical Engineering Science,* 61:4:1146-1156.

Chapter 4: Conclusion

4.1 Summary of Results

We studied gravure as an industrially viable process for printed electronics. In gravure printing, an engraved cylinder is submerged in an ink fountain and then rolled over a flexible substrate such as plastic or paper. A tightly pressed blade, called the doctor blade, wipes off excess ink from the non-image areas of the cylinder surface before contact with the substrate. We chose gravure because it is a mechanically simple process with fewer controlling variables than competing high-speed printing processes. Gravure has high throughput, long print runs, uniformity, and versatility.

We also explored the construction of a custom gravure printing system. We discussed the design of a laboratory size printer and compared it to an industrial size printer. The laboratory printer is designed to use only a small amount of ink per print and to align successive prints within 2 microns. Its main disadvantage is its inability to print at high speeds. However, the printing trends discovered with this printer should be transferable to an industrial scale printer, because the basic principles of printing remain the same.

We also discussed techniques to optimize the gravure cylinder. We chose to use copper-chrome cylinders because of their reliability and prevalence in the industry. We identified a number of cylinder metrics necessary for good printing, including TIR, taper, and surface roughness. *Rz* is a measure of the average peak-to-valley roughness and is the most commonly cited metric for identifying acceptable cylinders. For optimal wiping of nanoparticles, the cylinder must be cross-polished with an *Rz* of 200 nm. With regards to patterning cylinders, the most successful method in this project was the indirect laser method. The minimum achieved cell size was 11-15 microns wide, with a depth of 4 microns. For optimal printing results, the cell size uniformity must be improved.

Next, we considered the theoretical considerations necessary to develop a printing process to deposit conductive lines less than 20 microns wide, suitable for bottom-gate thin film transistors (TFTs). We identified a number of important factors for cell emptying and drop spreading, including the cell width, cell aspect ratio, print speed, ink viscosity, and substrate surface energy. We demonstrated gravure-printed nanoparticle

lines and presented techniques for optimizing the printed line quality. The minimum line width achieved was 30 microns, although these lines are currently not suitable as gate lines because of width and height nonuniformities resulting from cell size variation. In order to further scale our printed lines, we must either decrease the minimum cell size or decrease the wetting of the ink on the substrate.

4.2 Future Work

The future work can be divided into two main areas: improving roll patterning and modifying ink/substrate surface energies. First, the patterning uniformity must be improved, such that the cell size variance is less than a micron. Additionally, the minimum cell size must be scaled to at least 5 microns or below. One possible solution to both these requirements is to develop a dry etching process for the cylinder surface, which will involve developing a new plating and plasma etching technology.

Second, this report has studied only one type of silver nanoparticle ink on a single plastic substrate. Further experiments should be conducted with new nanoparticle inks and substrates. The amount of wetting can be decreased by either decreasing the substrate surface energy or increasing the ink surface tension, while still maintaining a reasonable cell emptying. We may want to also further explore the range of dilutions between ANP 50% and ANP 75%.

The current printing process should also be tested at faster printing speeds to bring it closer to an industrial process. Although print speed was identified as an important factor in cell emptying, it was not studied in this report. Increasing the print speed may also further minimize the achievable line width, since less ink tends to be put down on the substrate at faster speeds.

Overall, gravure printing is a promising technology that has many of the characteristics necessary for an industrially viable process for printed electronics. This report lays the foundation for future studies on roll-to-roll printed electronics, which will help to usher in a world where low-cost printed electronics become ubiquitous and a host of new applications are enabled.

Appendix A: Measurement Techniques

The Alpha-Step IQ Surface Profiler (ASIQ) and the Wyko NT3300 Profiling System (WYKO) were used to characterize the cylinder cells and printed features. The ASIQ is a contact profilometer with a 5 micron wide scanning stylus and a vertical resolution of about 50 nm. The WYKO is an optical interferometer with two measurements techniques: phase-shift interferometry (PSI) that uses a single wavelength of light, and vertical-scanning interferometry (VSI) that uses multiple wavelengths of light. The WYKO has a lateral resolution of about 600 nm and a vertical resolution of 1 nm for PSI mode and10-30 nm for VSI mode.

Figure A1 shows two cross-sections of an electromechanically engraved cell on the IGT roll using VSI mode, while Figure A2 shows a 3D image of a printed silver nanoparticle line. The 3D images allows for easy measurement of printed line width and height, as well as detailed assessment of the surface topology.

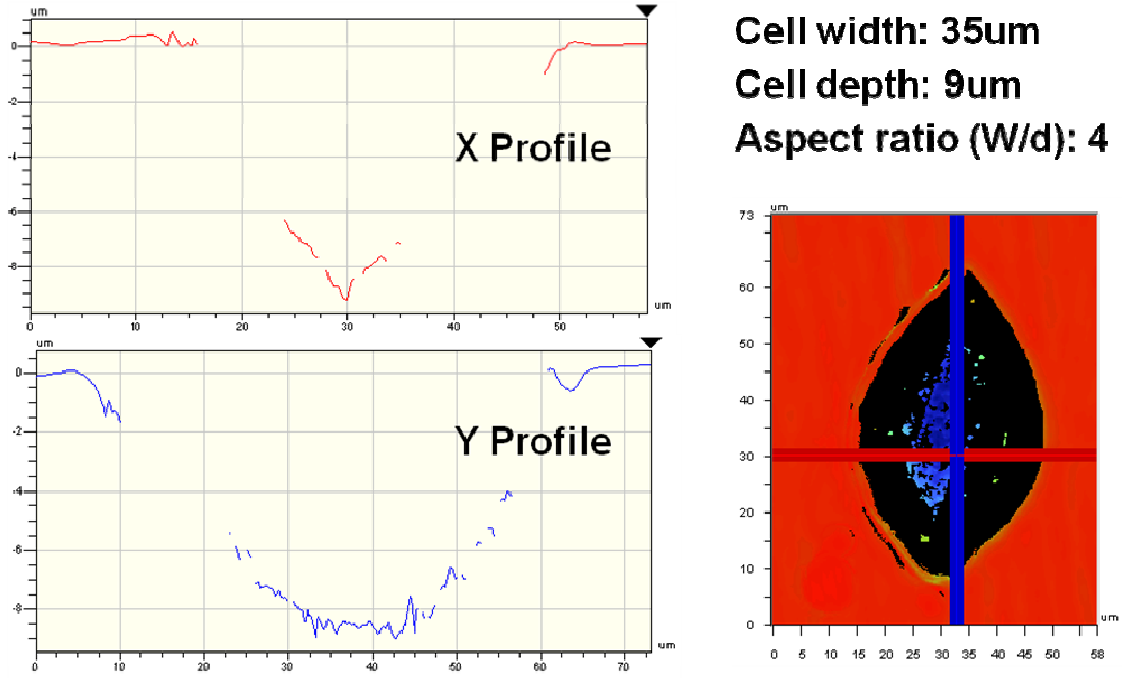

Figure A1. WYKO image of Electromechanically Engraved Cell (VSI mode)

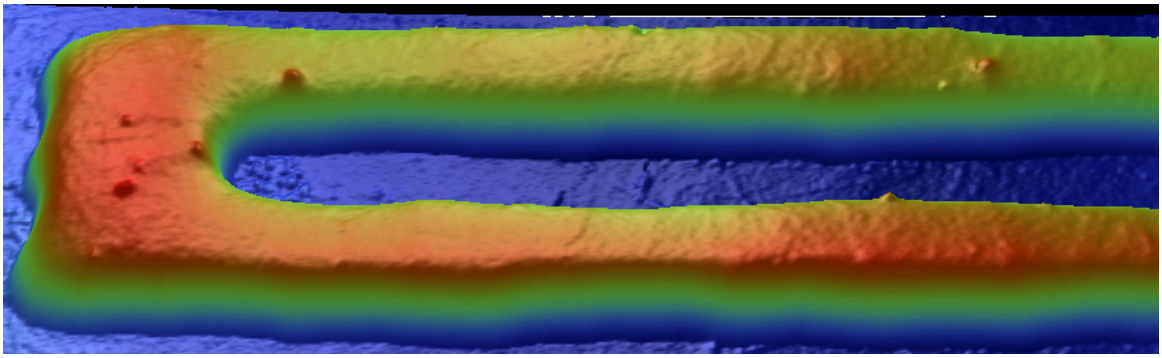

Figure A2. WYKO image of Printed Line (PSI mode)

One complication with the above image is that the WYKO is designed to make measurements on only one type of material at a time, so the WYKO's measured step heights of silver on plastic will not be correct. This discrepancy was corrected by correlating the WYKO and ASIQ heights, since the ASIQ height will not be affected by the choice of two different materials. We were able to obtain very similar profiles between both the ASIQ and WYKO, as shown in Figure A3.

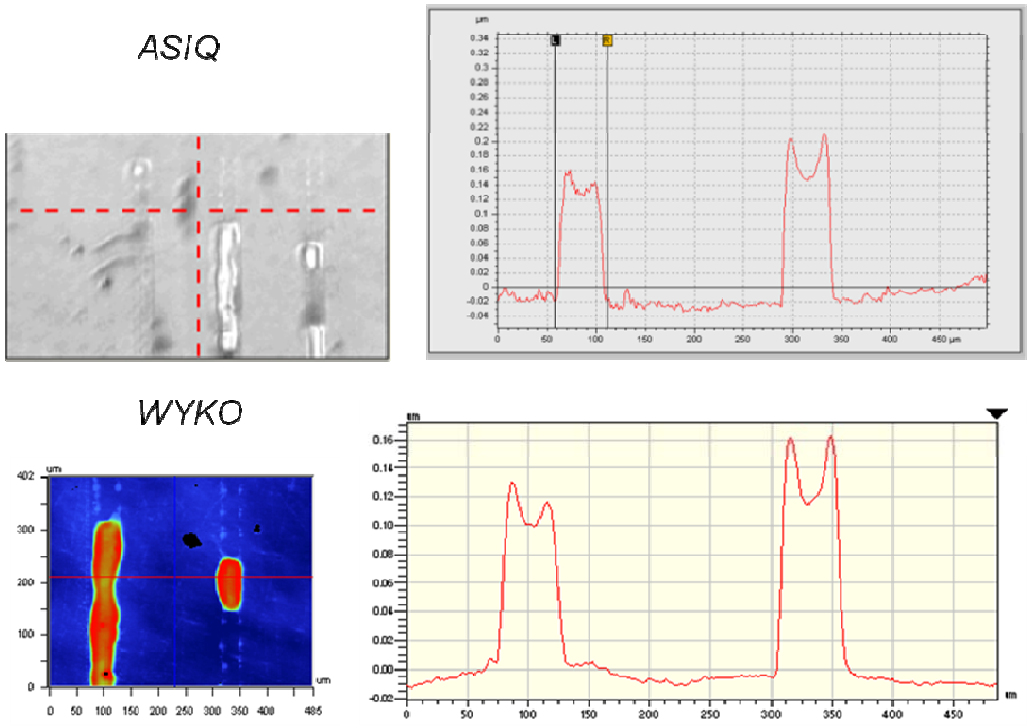

Figure A3. Comparison of ASIQ and WYKO profiles

As shown in Figure A4, the ASIQ height is approximately 50 nm greater than the measured WYKO height across a wide range of measurements. This allows us to make the simple assumption that the actual surface height is simply 50 nm greater than the measured WYKO height.

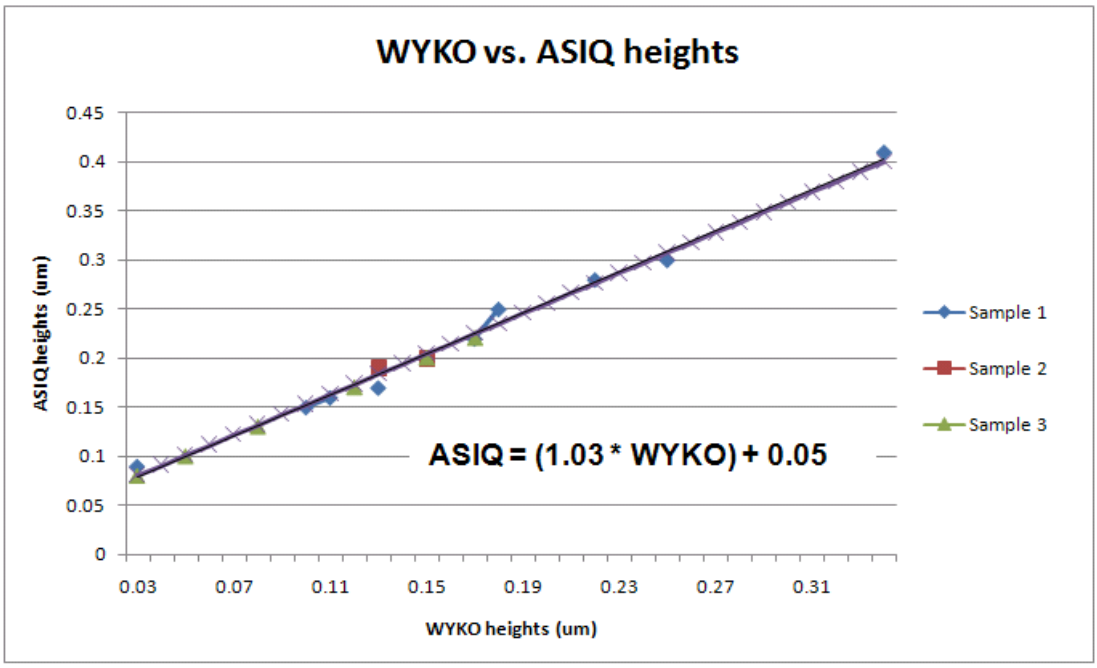

Figure A4. WYKO vs. ASIQ heights

Appendix B: Electrical Data

We printed four point probes in order to characterize the electrical performance of the ANP silver nanoparticle ink. The samples were printed on Melinex PET, a polymer made by Dupont Teijin Films, and were annealed at 150°C for 30 minutes on precision heating chucks. The nanoparticle ink is typically annealed at higher temperatures ranging from 150-250°C, but we are limited by the PET substrate, which becomes unacceptably deformed when annealed at temperatures above 150°C.

A set of printed four-point structures is shown in Figure B1. The lines are around 90 microns in width and 0.22 microns in thickness. The measured resistivity was about 4E-5 Ohm-cm, which is one order of magnitude greater than the given resistivity of 2E-6 Ohm-cm. This is not too surprising given that the ink was sintered at only 150°C. Despite the higher resistivity, the printed lines are still conductive enough to serve as gate lines.

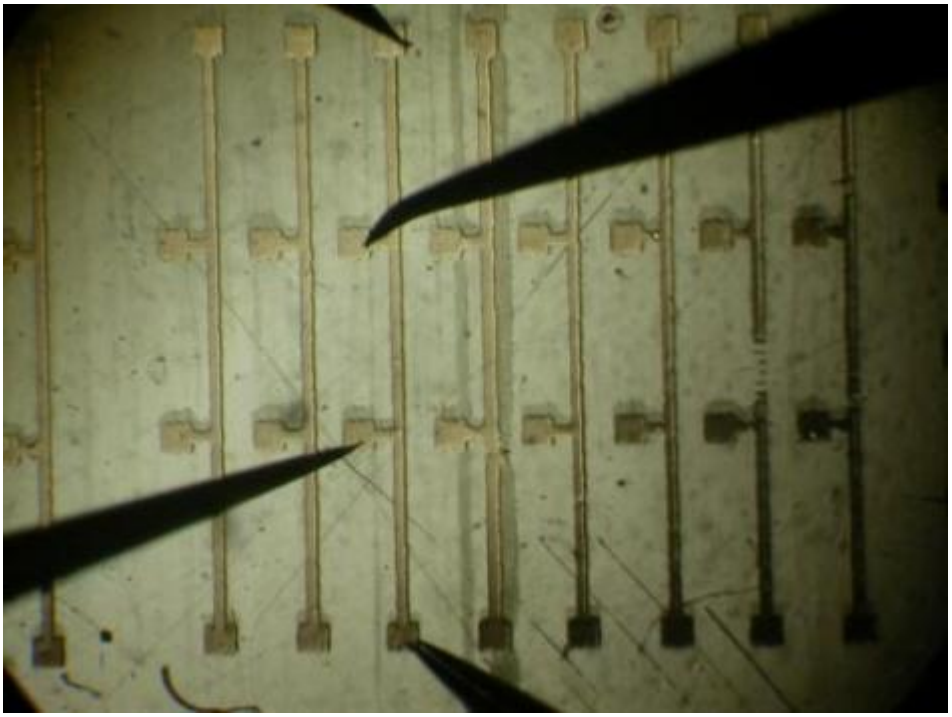

Figure B1. Printed Four-Point Structures with ANP Silver Nanoparticle Ink